Journal of Volcanology and Geothermal Research 412 (2021) 107192

Contents lists available at ScienceDirect

Journal of Volcanology and Geothermal Research

journal homepage: www.elsevier.com/locate/jvolgeores

Post-collisional shift from polygenetic to monogenetic volcanism revealed by new $^{40}Ar/^{39}Ar$ ages in the southern Lesser Caucasus (Armenia)

Patrick Sugden [a], Khachatur Meliksetian [b], Ivan P. Savov [a,*], Dan Barfod [c], Marjorie Wilson [a], Charles Connor [d], Gevorg Navasardyan [b], Edmond Grigoryan [b], David Manucharyan [b,d]

[a] Institute of Geophysics and Tectonics, School of Earth and Environment, University of Leeds, Leeds LS2 9JT, UK
[b] Institute of Geological Sciences, National Academy of Sciences of Armenia, 24a Marshal Baghramian Avenue, Yerevan 0019, Armenia
[c] NEIF Argon laboratory, Scottish Universities Environmental Research Centre, Rankine Avenue, Scottish Enterprise Technology Park, East Kilbride, G75 0QF, Scotland, UK
[d] School of Geoscience, University of South Florida, 4202 E. Fowler Avenue, NES 107, Tampa, FL 33620-555, USA

ARTICLE INFO

Article history:
Received 13 September 2020
Received in revised form 18 January 2021
Accepted 25 January 2021
Available online 31 January 2021

Keywords:
$^{40}Ar/^{39}Ar$ dating
Post-collisional volcanism
Monogenetic volcanoes
Lesser Caucasus

ABSTRACT

The post-collisional Syunik and Vardenis volcanic highlands, located in the southern Lesser Caucasus mountains (part of the Arabia-Eurasia collision zone) are host to over 200 monogenetic volcanoes, as well as 2 large Quaternary polygenetic volcanoes in the Syunik highland. The latter are overlain by lavas from the monogenetic volcanoes, suggesting there was a transition in the style of volcanic activity from large-volume central vent eruptions to dispersed small-volume eruptions. 12 new high quality $^{40}Ar/^{39}Ar$ ages are presented here, with 11 ages calculated by step-heating experiments on groundmass separates, and the final age obtained from total fusions of a population of sanidines. All the ages were younger than 1.5 Ma, except for one ignimbrite deposit whose sanidines gave an age of 6 Ma. While the bulk of the exposed products of post-collisional volcanism relate to Pleistocene activity, it is clear there has been active volcanism in the region since at least the late Miocene. All ages for monogenetic volcanoes in the Syunik highland are younger than 1 Ma, but to the north in Vardenis there is geochronological evidence of monogenetic volcanism at 1.4 and 1.3 Ma. An age of 1.3 Ma is determined for a lava flow from one of the polygenetic volcanoes- Tskhouk, and when combined with other ages helps constrain the timing of the polygenetic to monogenetic transition to around 1 Ma. The new ages illustrate a degree of spatio-temporal coupling in the formation of new vents, which could be related to pull-apart basins focussing ascending magmas. This coupling means that future eruptions are particularly likely to occur close to the sites of the most recent Holocene activity. The polygenetic to monogenetic transition is argued to be the result of a decreasing magma supply based on: (i) volume estimates for Holocene eruptions and for all monogenetic volcanoes and their lava flows in Syunik; and (ii) the volcanic stratigraphy of the Lesser Caucasus region which shows late Pliocene- early Pleistocene continental flood basalts being succeeded by a few large andesite-dacite volcanoes and then the most recent deposits consisting of small-volume scoria cones. The Syunik highland has the highest density of monogenetic centres in the Lesser Caucasus, which is taken to indicate this region has the highest magma flux, and was therefore the last location to transition to monogenetic volcanism, which is why the transition is most clearly seen there. There is no evidence from Sr-Nd-B isotope measurements for the exhaustion of fusible slab components in the mantle source, showing that an inherited slab signature can survive for millions of years after the end of subduction. Although volcanism in the Lesser Caucasus is currently waning, a future pulse of activity is possible.

1. Introduction

The most fundamental classification of volcanoes is the distinction between polygenetic and monogenetic edifices (Rittmann, 1962; Nakamura, 1977;). Polygenetic volcanoes are constructed from successive eruptions through a stable central conduit. The resulting volcanic stratigraphy includes clear breaks in the geological record between deposits of multiple eruptive cycles (e.g. Luhr et al., 2010). In contrast, monogenetic volcanoes are defined as only having one eruptive episode, which can last anything from hours to decades (Smith and Németh, 2017). Monogenetic volcanoes are distinguished from polygenetic volcanoes based on their geomorphology, being usually much smaller volume and simpler in form, indicating a comparatively brief eruptive history

* Corresponding author.
E-mail address: I.Savov@leeds.ac.uk (I.P. Savov).

https://doi.org/10.1016/j.jvolgeores.2021.107192

(e.g. Yokoyama, 2019). Despite not representing the archetypal image of a volcano, monogenetic volcanoes are found at every plate boundary and intraplate setting at which polygenetic volcanoes form (Hildreth, 2007; Thordarson and Larsen, 2007; Kiyosugi et al., 2010; Mazzarini and Isola, 2010; Dóniz-Páez, 2015; Muirhead et al., 2016; Reynolds et al., 2018; Bertin et al., 2019; Gómez-Vasconcelos et al., 2020). Although the eruptive lifetime of a single monogenetic volcano is relatively short, they normally form part of a larger structure of multiple monogenetic volcanoes known as a volcanic field. Such fields can have lifespans as long as, if not longer than polygenetic volcanoes. The mode of volcanic activity which leads to the formation of these structures is sometimes referred to as "distributed volcanism" (Valentine and Connor, 2015).

Polygenetic volcanism from a single central vent and monogenetic volcanism in a distributed volcanic field are actually end members of a spectrum of volcanic activity and landforms. Transitional styles include large volcanic complexes with polygenetic eruptive vents and numerous parasitic cones, often extending tens of kilometers away from the base of the larger volcano. This is an extremely common style of activity, as the recent eruptions of monogenetic vents in the Tolbachik volcano group (Kamchatka) demonstrate (Belousov et al., 2015). As such, some researchers have argued for a second petrogenetic criterion, whereby a monogenetic volcano is fed by a discrete mantle-derived batch of magma, and not a mature interconnected plumbing system (Smith and Németh, 2017). However, the complex interconnected relationship between dykes and monogenetic volcanoes in volcanic fields such as San Rafael (Utah, USA) and Hopi Buttes (Arizona, USA) suggests this criterion is problematic (Kiyosugi et al., 2012; Muirhead et al., 2016). For simplicity, in this contribution we use the term monogenetic only in the volcanological sense.

Why do these differences occur in the distribution of volcano landforms and their types? A low magma supply rate, a high rate of crustal extension or a combination of the two are the most commonly cited explanations for distributed volcanism (Nakamura, 1977; Fedotov, 1981; Walker, 1993; Takada, 1994a). Low magma supply has been suggested to prevent the continued existence of a "hot pathway" for magmas to propagate to the surface (Fedotov, 1981; Walker, 1993). Most volcanic fields have eruption recurrence rates on the order of 10^{-5} to 10^{-4} eruptions/year (Valentine and Connor, 2015), which is a low rate of activity in comparison to typical stratovolcanoes (Luhr et al., 2010). The cause of the link between monogenetic volcanism and high rates of crustal extension is less clear. It has been suggested that high rates of crustal extension prevent dyke coalescence and magma mixing (Takada, 1994b), or else they promote lateral transport and retard magma focussing (Nakamura, 1977). Whatever the cause, it is clear that distributed volcanism is favoured in regions of high extension (e.g. Takada, 1994a; Bucchi et al., 2015).

Despite requiring different magma supply rates or local tectonic stress regimes, monogenetic and polygenetic volcanoes are often found in surprisingly close proximity (within a few km; Nakamura, 1977; Settle, 1979; Bucchi et al., 2015; Germa et al., 2019; Riggs et al., 2019; Sieron et al., 2019a). The Lesser Caucasus, located largely in the country of Armenia and within the Arabia-Eurasia collision zone, is one such region that hosts both polygenetic and monogenetic volcanoes (Fig. 1). Polygenetic volcanoes include Aragats (> 3 km tall with a 42 km basal diameter; 1.8–0.5 Ma; Gevorgyan et al., 2018), Ararat (~4 km tall with a 40 km basal diameter; 1.5–0.02 Ma; Yilmaz et al., 1998), Tskhouk and Ishkhanasar (Fig. 1). Across the Lesser Caucasus region (Fig. 1), there are 772 mapped monogenetic volcanoes in Armenia, easternmost Turkey and southern Georgia, all of which formed since 11 Ma, with the vast majority produced in the last few million years (Keskin et al., 2006; Arutyunyan et al., 2007; Connor et al., 2011; Lebedev et al., 2013). This gives an average density of vents for the Lesser Caucasus of ~0.016 per km^2. For comparison, the Baja California field, NW Mexico, which is considered to be one of the densest clusters of volcanoes on earth, contains 900 vents, formed between 12.5 and < 1 Ma, with a density of 0.013 vents per km^2 (Germa et al., 2013). Many of these monogenetic volcanoes are found in volcanic highlands such as the Erzurum-Kars Plateau and the Gegham, Vardenis and Syunik highlands, or on the flanks of large polygenetic volcanoes such as Aragats and Ararat (Fig. 1).

Both types of volcano present their own distinct hazards to local populations and infrastructures. Polygenetic volcanoes have the potential to produce larger (in volume) and more explosive eruptions, whose effects will cover the widest areas. Eruptions from monogenetic volcanoes are likely to affect a smaller area but are much more unpredictable in terms of their location. Within the Lesser Caucasus region, the Armenian nuclear power plant (Karakhanian et al., 2003; Connor et al., 2011, 2012; IAEA-TECDOC-1795, 2016), the city of Yerevan with a population of over 1.2 million (Lebedev et al., 2013; Gevorgyan et al., 2018), and the M2 road link between Iran and the Caucasus (Karakhanian et al., 2002; Sugden et al., 2019) are all located within a few km of both monogenetic and polygenetic volcanoes. This means understanding the nature of the volcanic hazard in this region is of substantial geopolitical significance for Armenia and the surrounding countries.

An area of particular interest is the Syunik volcanic highland (Fig. 1), which is host to 160 monogenetic volcanic centres, and two polygenetic volcanoes- Tskhouk and Ishkhanasar. The most recent Holocene activity in Syunik involved a cluster of monogenetic cones (Karakhanian et al., 2002), while Tskhouk and Ishkhanasar appear to be inactive. This leads one to the hypothesis that there has been a shift over time from polygenetic to monogenetic volcanism in Syunik.

We test this hypothesis by presenting a new set of high quality $^{40}Ar/^{39}Ar$ ages for key volcanic units from Syunik. These ages are used in conjunction with previous K—Ar (Karapetian et al., 2001; Ollivier et al., 2010), $^{40}Ar/^{39}Ar$ (Joannin et al., 2010; Meliksetian et al., 2020) and apatite fission track ages (Karapetian et al., 2001) to make some conservative estimates of the recurrence interval of eruptions; and to constrain the timing of the polygenetic to monogenetic transition. The age data are combined with geochemical and geospatial data for Syunik in order to investigate the origin of the transition, i.e. whether it was related to a decreasing magma supply or increased crustal extension. Two samples from Vardenis (just to the north of Syunik; Fig. 1) were also $^{40}Ar/^{39}Ar$ dated to test the geographical extent of any polygenetic- monogenetic transition and whether or not it occurs contemporaneously.

2. Geological setting and previous age constraints

Syunik volcanic highland is located on the Anatolian-Armenian-Iranian plateau, a broad uplifted region formed by the northward indentation of the Arabian plate into the Eurasian plate. The ~500 km wide plateau is the only continent-continent collision setting on Earth which hosts widespread and volumetrically significant Quaternary post-collisional volcanism (Fig. 1), although there are a couple of rare cases of Quaternary volcanism on the Tibetan plateau as well (Zou et al., 2020a, 2020b). Volcanism appears to have initiated in the late Miocene (Keskin et al., 1998; Keskin, 2003; Arutyunyan et al., 2007; Şengör et al., 2008), although perhaps not until <5 Ma in the south of the plateau (Keskin, 2003). Volcanism has been variously attributed to slab break-off (Keskin, 2003), small-scale lithospheric delamination (Kaislaniemi et al., 2014), amphibole dehydration melting (Allen et al., 2013), or various combinations of these factors (Neill et al., 2015; Sugden et al., 2019).

Post-collisional volcanism is not a minor feature of the plateau, with eastern Anatolia alone being covered by ~15,000 km^3 of post-Miocene lavas, ignimbrites and other eruptive products (Şengör et al., 2008). Across the plateau, there are examples of both polygenetic and monogenetic volcanism. Polygenetic volcanoes include those surrounding Lake Van (Nemrut, Suphan and Tendurek), as well as volcanoes such as Sabalan in NW Iran (Yilmaz et al., 1998; Ghalamghash et al., 2016). Examples of monogenetic centres include the Erzurum-Kars plateau in eastern Anatolia, and the small volcanoes of the Kurdistan province of NW Iran (Keskin et al., 1998; Allen et al., 2013).

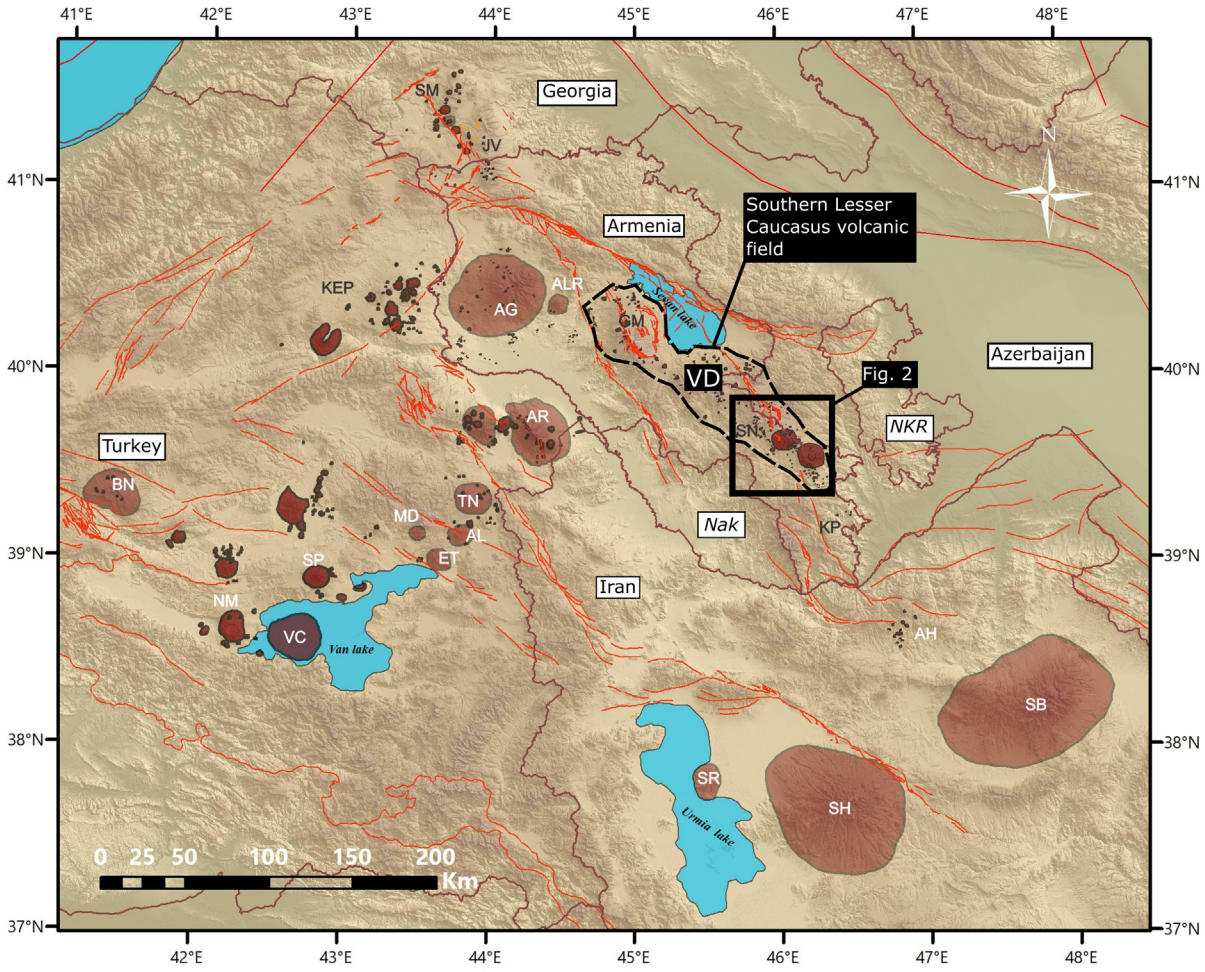

Fig. 1. Distribution of Quaternary volcanoes in the central part of the Anatolian-Armenian-Iranian plateau. The large brown coloured regions give the locations of polygenetic volcanoes, while the clusters of smaller spots show the locations of volcanic fields. The southern Lesser Caucasus volcanic field is outlined by the black dashed line. The area covered by the map of the Syunik highland shown in Fig. 2 is shown by the black box, with the Vardenis highland just to the north-west, labelled by the black box as "VD". Volcano name abbreviations: AG – Aragats; AL – Aladag; ALR – Arailer; AR- Ararat; AH- Ahar volcanic field; BN – Bingol; ET – Etrusk; GM – Gegham volcanic highland; KEP – Kars-Erzerum volcanic plateau; JV- Kechut – Javakhk volcanic plateau; KP- Kapan volcanic highland; MD – Meydan Dag; NM – Nemrut; SB – Sabalan; SH – Sahand; SM – Samsari volcanic field; SN – Syunik volcanic highland; SP – Sipan (Süphan); SR- Saray; TN – Tondrak (Tendurek); VC – Van caldera. Active faults after Karakhanyan et al. (2016). The outlined area labelled "NKR" refers to the disputed Nargorno-Karabakh region, while the area labelled "Nak" is Nakhichevan is an autonomous region that is part of Azerbaijan. (For interpretation of the references to colour in this figure legend, the reader is referred to the web version of this article.)

As can be seen in Fig. 1, the Syunik volcanic highland is located towards the northern edge of the Anatolian-Armenian-Iranian plateau, yet in a central position between the volcanoes of eastern Anatolia and NW Iran. In terms of the monogenetic volcanism, it can be considered the south-eastern end of the southern Lesser Caucasus volcanic field (Fig. 1). This field consists of the Gegham, Vardenis and Syunik volcanic highlands referred to in Sugden et al. (2019). In this contribution we focus on the Syunik region because it hosts both polygenetic and monogenetic volcanoes, the previous paucity of age data, and the potential for use of a geothermal energy source due to documented Holocene activity (White et al., 2015). We also explore for evidence from the volcanic stratigraphy of the Vardenis highland to the north of Syunik (Fig. 1), to determine whether a polygenetic to monogenetic transition in Syunik extends to the north- towards the capital of Armenia, Yerevan (Fig. 1; Connor et al., 2012; Gevorgyan et al., 2018).

Both Vardenis and Syunik host a large number of monogenetic volcanic centres. The size and morphology of these volcanic centres is typical of monogenetic volcanoes worldwide. The height, basal diameter, and crater diameter of a selection of volcanoes from the studied region are shown in Table 1. The examples of the southern Lesser Caucasus volcanoes include those that are both larger and smaller than the famous Parícutin volcano, Mexico, which is known to have formed by a single eruption from 1943 to 1952 (Foshag and González Reyna, 1956). In contrast, one of the polygenetic volcanoes, Ishkhanasar, is an order of magnitude larger (Table 1), and clearly must have formed through multiple eruption cycles.

2.1. Syunik volcanic highland

Syunik hosts a minimum of 160 volcanic centres composed of mafic-intermediate scoria cones and lavas, as well as rhyolite domes (Meliksetian, 2013). A recently completed geological map indicates that the polygenetic volcanoes are older than the monogenetic volcanoes in Syunik (Fig. 2). Close to the base of the volcanic section is the Goris strata debris avalanche volcaniclastic deposit, which formed due to the collapse of a large (likely polygenetic) volcanic edifice. It is thought to be upper Pliocene in age given that it lies directly below the lower Pleistocene Sisian suite sediments in the Tatev Gorge (southern boundary of the mapped region in Fig. 2). These lacustrine diatomite sediments are in turn capped by lava flows from nearby monogenetic volcanoes (Fig. 2; Ollivier et al., 2010). Two polygenetic edifices are still observable in Syunik: Ishkhanasar (in the SE) and Tskhouk (to the

Table 1
Morphological characteristics for several of the best-preserved volcanoes in the southern Lesser Caucasus. Also shown for comparison is one of the best known monogenetic volcanoes, Parícutin.

Volcano Name, and highland	Coordinates, WGS-84, Decimal Degrees		Diameter of the base, m	Diameter of the crater, m	Altitude, a.s.l. m	Relative elevation, m
	Lat	Long				
Karkar, Syunik	39.749824° N	45.953640° E	2100	–	3208	308
Tsakkar, Syunik	39.717606° N	46.002000° E	1220	340	3197	174
Nazeli, Syunik	39.715842° N	46.008595° E	330	110	3154	51
Paytasar, Syunik	39.722585° N	46.008059° E	490	160	3119	37
Mets Erkvoryak, Syunik	39.637170° N	46.120621° E	1491	470	2838	190
Merkasar, somma volcano in caldera of Ishkhanasar, Syunik	39.579161° N	46.234376° E	3250	–	3233	523
Ishkhanasar stratovolcano, Syunik	39.579905° N	46.180706° E	23,000	7100 (caldera)	3550	1527
Porak, Vardenis	40.029096° N	45.739295° E	1230	310	3046	246
Torgomayir, Vardenis	39.987532° N	45.612497° E	1363	–	3451	140
Karmravor, Vardenis	40.118624° N	45.561915° E	1460	300	2377	158
Vayotsar, Vardenis	39.798051° N	45.499641° E	1587	510	2586	589
Parícutin, Trans-Mexican volcanic belt- erupted in 1943	19.49306° N	102.2514° W	870	275	2800	208

NW; Fig. 3a). Lava flows associated with these polygenetic volcanoes are sometimes covered by the volcanic deposits of monogenetic volcanoes. For example, the Sherepasar monogenetic volcano clearly formed on top of the pre-existing lava flows from Tskhouk polygenetic volcano (Fig. 3b). Similarly, the calderas of Ishkhanasar and Tskhouk are host to younger monogenetic somma volcanoes. Merkasar is a 3 km diameter, 500 m high somma dated to 0.7 ± 0.1[1] Ma (K—Ar), nested in the south-east facing caldera of Ishkhanasar (Karapetian et al., 2001).

$^{40}Ar/^{39}Ar$ ages of 1.16 ± 0.02 and 1.24 ± 0.03 Ma have been obtained for volcanic tephra layers interbedded with diatomite sediments in the Sisian suite (Joannin et al., 2010). The large clast size (described as "conglomeritic" with cm-sized pumice clasts) and the thickness of these deposits (1–2.5 m), suggests the volcanic material could be derived from a proximal source (Joannin et al., 2010). A significant magma chamber, with a sufficient magma volume to force a mass eruption rate high enough to drive a Plinian eruption would usually require a local polygenetic volcano to erupt this tephra deposit.

Ages from monogenetic volcanoes in Syunik are exclusively younger than 1 Ma. Several lava flows from monogenetic volcanoes that cap these sedimentary sequences have all been dated at <1 Ma using the K—Ar technique (Ollivier et al., 2010). Several monogenetic rhyolite domes and lava flows have been dated to 0.9–0.3 Ma using apatite fission track (AFT) and K—Ar methods (Fig. 2; Karapetian et al., 2001). The Karkar group of volcanoes, located to the north of Tskhouk volcano in a pull-apart basin at the southern termination of the Pambak-Sevan-Syunik fault (Fig. 2) were active into the Holocene (Fig. 3d). Archaeological evidence suggests the most recent eruptions occurred around 5 ka (Karakhanian et al., 2002). Four new $^{40}Ar/^{39}Ar$ ages from the Karkar group give ages of 14–9 ka (Meliksetian et al., 2020).

2.2. Vardenis volcanic highland

The volcanic stratigraphy discussed here is based on fieldwork conducted for this study and radiometric ages from the literature. Large ignimbrites form the base of the volcanic sequence (Fig. 3c), attesting to the presence of large, likely caldera-forming, volcanoes early in the volcanic history of the region. Above the ignimbrites are a succession of lava flow units which are mafic at the base, but grade into trachydacites up-section. A trachydacite from one of these volcanic peaks (Sandukhansar) has a K—Ar age of 3.7 ± 0.4 Ma (Karapetian et al., 2001). The substantial size of these edifices (up to 10 km across, ~700 m relative elevation) might suggest they were polygenetic volcanoes.

Choraphor is a rhyolite dome (~2 km diameter) on the northern slopes of the Vardenis ridge; obsidians from this dome give a K—Ar age of 1.75 Ma (Karapetian et al., 2001). Its reduced size when compared to the Pliocene dacites is an indication of comparatively short-lived eruptive activity. While investigating the long term slip rate on the Pambak-Sevan-Syunik strike-slip fault, Philip et al. (2001) determined the age of the Khonarhasar scoria cone, which is dissected by the fault, leading to one half of the cone being offset along the fault from the other. Using the K—Ar technique, an age of 1.40 ± 0.03 Ma was established, showing definitively that Vardenis was host to some monogenetic volcanism by this date.

To the south of Khonarhasar, Porak (Fig. 3g) is a Holocene volcanic complex which has been interpreted as the youngest volcanic structure in Vardenis, and was the site of the most recent eruption in Armenia (~3 ka; Karakhanian et al., 2002). Porak is interpreted to have an eruptive history dating back to the middle Pleistocene, but which includes multiple generations of Holocene lava flows (Karakhanian et al., 2002). The co-incidence of widespread forest fires, a large earthquake, and local rock carvings (petroglyphs) depicting volcanic eruptions, all dated to ~6500 yrs. BP, suggests an eruption at this time (Karakhanian et al., 2002). A later eruption at ~2800 yrs. BP is indicated on the basis of historical accounts of a military campaign, as well as radiocarbon dating of the walls of a town cross-cut by the youngest generation of lava (Karakhanian et al., 2002). The Porak volcanic system has clearly hosted multiple eruptions. However, rather than being a single, central volcanic cone, Porak can also be interpreted as a group of monogenetic volcanoes. The Holocene eruptions were fed from cones on the flank of Porak rather than the summit (Karakhanian et al., 2002). There are 10 cones mapped in the Porak region, and similar to the Karkar volcanoes in Syunik, this region is bounded by strike-slip faults that form a pull-apart basin. Although the volcanoes of the Porak and Karkar groups are monogenetic, these clusters are both supplied by long-lived magmatic systems.

Two of the other youngest volcanoes in Vardenis are Vayots Sar (Fig. 3f) and Smbatassar (late Pleistocene to Holocene based on underlying river terraces; Karakhanian et al., 2002). These volcanoes are located in the south-west of the Vardenis highland, 17 km apart from each other. They are relatively isolated from other recent activity and quite clearly represent monogenetic activity. Their isolation also illustrates the unpredictability of the hazard posed by monogenetic volcanism, in terms of considering where the next eruption is most likely to occur.

The evidence available suggests that early volcanism in Vardenis produced caldera-collapse ignimbrite-forming eruptions from polygenetic

[1] Uncertainty not reported, but it is estimated here and for other ages from this publication as ~ ± 10% based on the average for those uncertainties which are reported for other K—Ar ages.

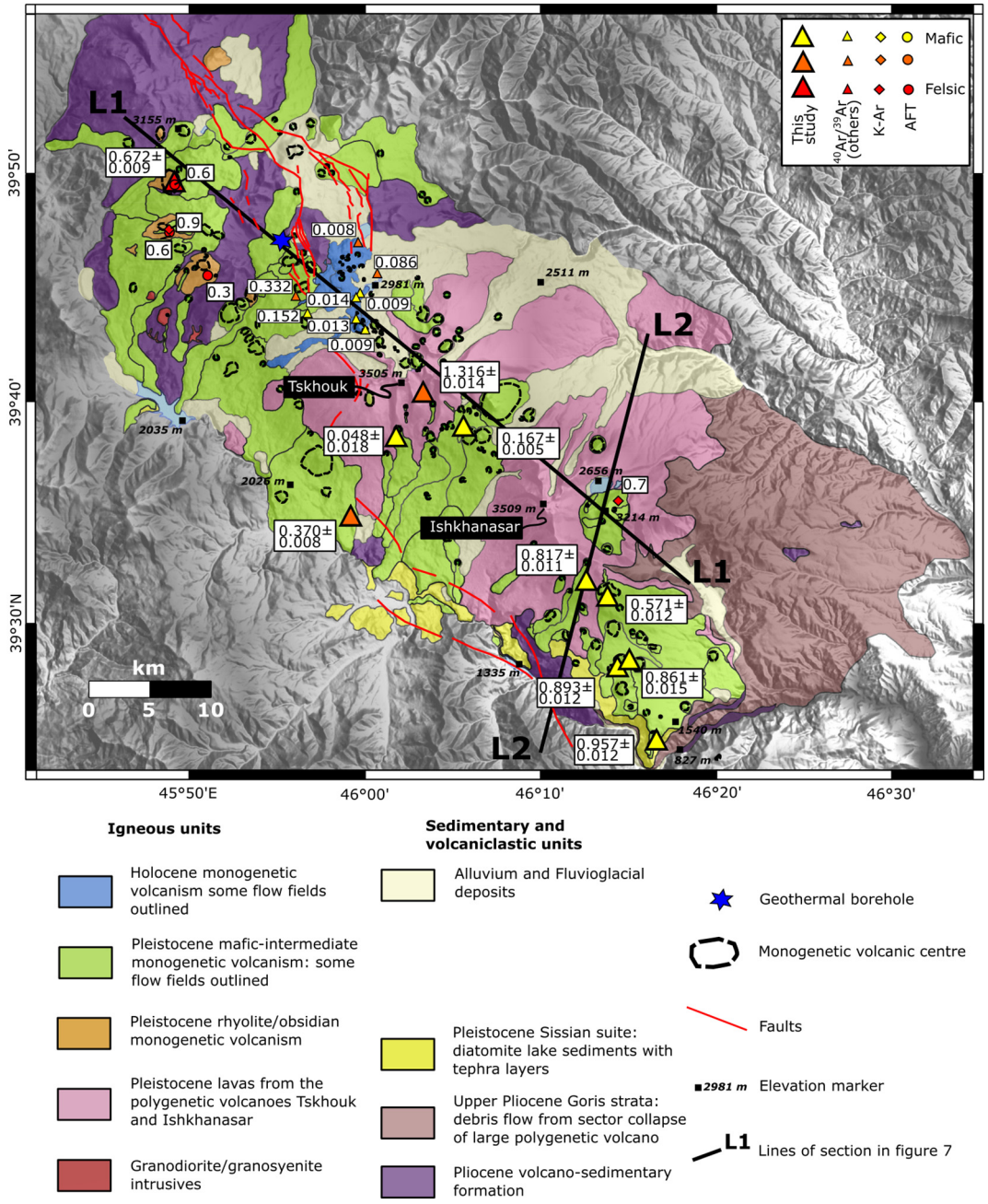

Fig. 2. Geological map of the Syunik volcanic highland, with the area of the map shown in Fig. 5.1b. Map modified from that shown in Sugden et al. (2019) and Meliksetian (2013). Samples are colour coded according to their composition and the shapes denote the method by which an age was obtained: ^{40}Ar/^{39}Ar, K—Ar, apatite fission tracks (AFT). ^{40}Ar/^{39}Ar age determinations for this study are shown by the large triangles with 2σ error. Also note the Sisian suite of lacustrine sediments shown in yellow, within which 2 tephra layers have been dated (1.24 ± 0.03 and 1.16 ± 0.02 Ma; Joannin et al., 2010), with several of the lava flows capping the sediment sequence also being dated (1–0.1 Ma; Ollivier et al., 2010). (For interpretation of the references to colour in this figure legend, the reader is referred to the web version of this article.)

volcanoes. The youngest volcanic activity has produced several monogenetic volcanoes around Porak, as well as the more isolated Vayots Sar and Smbatassar. Although the evidence is less clear than for Syunik to the south, it does appear that there was a polygenetic to monogenetic transition in Vardenis. Unlike in Syunik, where evidence for monogenetic volcanism is confined to the last 1 Ma, there is evidence of monogenetic volcanism stretching back to 1.4 Ma, and possibly 1.75 Ma (Karapetian et al., 2001; Philip et al., 2001).

3. Sample selection

Sample selection focussed predominantly on the Syunik volcanic highland for several reasons: (i) the evidence that this is a region where a transition from polygenetic to monogenetic volcanism occurred; (ii) the large number of mafic eruptive centres, which when age constrained can be used to look at the potential exhaustion of fusible components in the mantle source over time; (iii) the detailed geological map (Fig. 2) which allows ^{40}Ar/^{39}Ar ages to be related to the number of mapped monogenetic centres, such that recurrence intervals of volcanism can be investigated. Two samples from the Vardenis highland were also dated, to look at how constraints on the timing of any polygenetic to monogenetic transition compare with what is observed in Syunik.

In Vardenis, one basaltic trachyandesite lava (sample 6.3.15) and one ignimbrite (sample 5.1.15) were selected for dating. The lava is a small volume mafic eruption that lies directly on top of massive

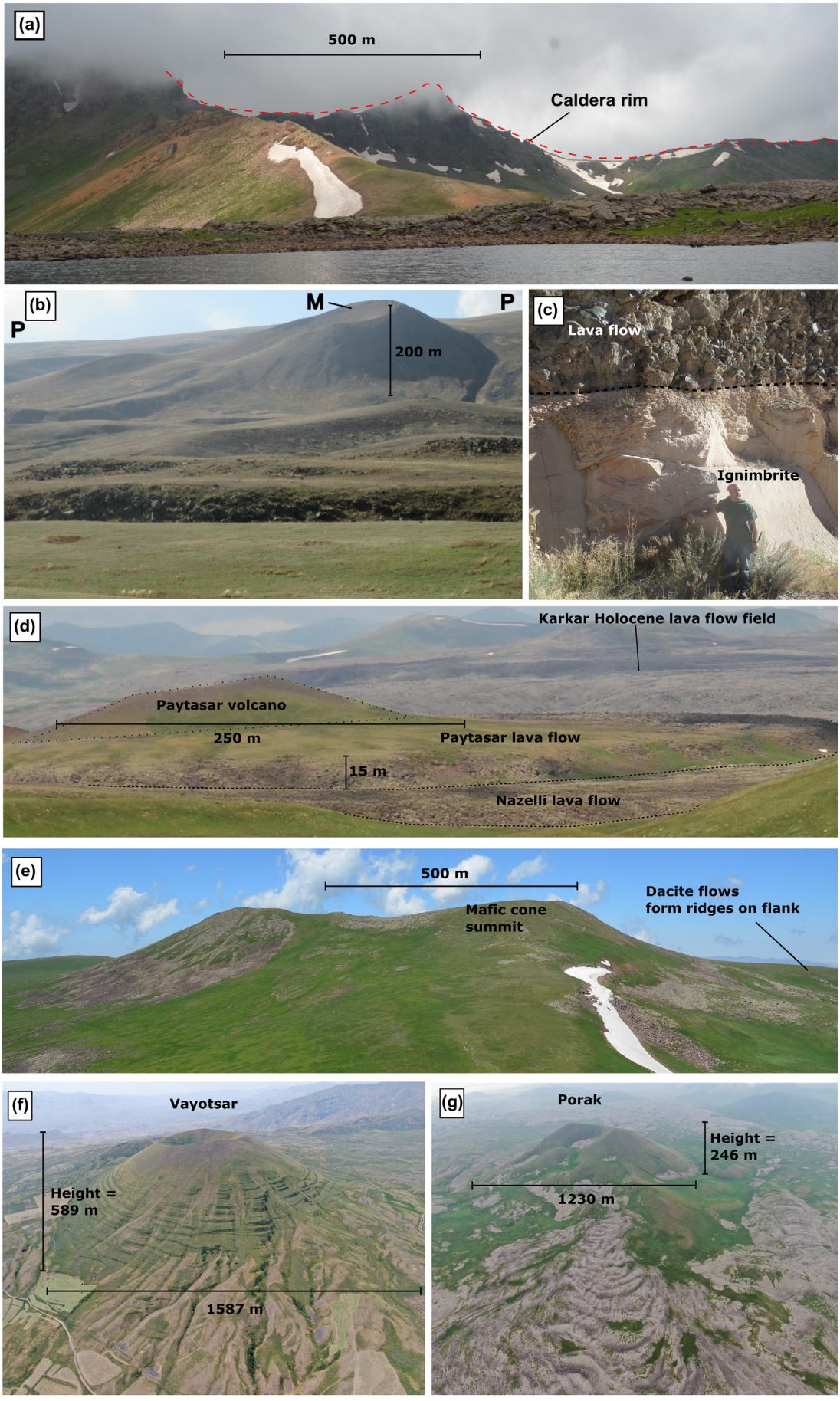
(a)
500 m
Caldera rim
(b)
M
P
P
200 m
(c)
Lava flow
Ignimbrite
(d)
Karkar Holocene lava flow field
Paytasar volcano
250 m
Paytasar lava flow
15 m
Nazelli lava flow
(e)
500 m
Mafic cone summit
Dacite flows form ridges on flank
(f)
Vayotsar
Height = 589 m
1587 m
(g)
Porak
Height = 246 m
1230 m

trachydacite lavas (Fig. 3e). These trachydacites are thought to have been erupted at ~3.7 Ma, based on a K—Ar age for a similar trachydacite ~3 km to the north (Karapetian et al., 2001). If this mafic lava is much younger than the trachydacites underneath it, then it can be considered monogenetic. If it formed at a similar time to the dacites then the case for a polygenetic volcanic system (capable of erupting several batches of magma of different compositions) at this time would be strengthened. The precise age could further constrain the timing of the poly- to monogenetic shift. The large ignimbrite unit at the base of the volcanic section provides an age for the basement on which all younger lava flows must have been built, and an age at which volcanic activity must have been polygenetic.

In Syunik, one sample is from a lava flow erupted from the Tskhouk polygenetic volcano (sample 5.5.12), while the other nine samples come from monogenetic centres. The age of the Tskhouk lava shows definitively when the polygenetic volcano must have been active. If the age is similar to the tephra layers in the diatomite sediments this would support the view that these tephra came from a local stratovolcano. It would also show that the polygenetic to monogenetic transition occurred later here than to the north.

The bulk of new ages presented are for monogenetic volcanoes in Syunik. Most of the samples have mafic compositions and have been analysed for Sr-Nd-B isotopes. This means the ages can be used to look at how the magma source may have changed over time, and whether there are any signs of it being depleted, which is one way in which a decreased magma supply might be revealed. It is possible that the polygenetic to monogenetic transition in Syunik represents an exhaustion of fusible subduction components in the mantle source. These mafic samples will be used to test this hypothesis.

4. Analytical methods

Samples were prepared for irradiation at the Scottish Universities Environmental Research Centre (SUERC). The groundmass fraction of most samples was used for $^{40}Ar/^{39}Ar$ analysis to avoid inherited argon and maximise the K content. Sample preparation followed a rigorous procedure, whereby samples were crushed to the 250–500 μm size fraction and leached for 30 min in 3 M HNO_3 in an ultrasonic bath to remove altered groundmass material. Following this, the grains were passed through a barrier-type Franz magnetic separator to remove phenocrysts. Final hand-picking removed any residual phenocrysts and altered groundmass to give 400 mg of purified separate.

For the ignimbrite sample (5.1.15), sanidine phenocrysts were used instead to obtain an age via total fusions of a population of single grains. Sanidine crystals were processed by crushing and magnetic separation, in the same way as for the groundmass samples. Sanidine was then separated using heavy liquid density separation, followed by a final magnetic separation to minimise the presence of inclusions. The sanidine crystals were leached in dilute HF to remove any pumice glass coating the grains. Hand picking was then used to select the most appropriate phenocrysts for analysis.

Samples and neutron flux monitors were packaged in copper foil and stacked in quartz tubes with the relative positions of packets precisely measured for later reconstruction of neutron flux gradients. The sample package was irradiated in the Oregon State University reactor, Cd-shielded facility. Alder Creek sanidine (1.1891 ± 0.0008 (1σ) Ma; Niespolo et al., 2017) was used to monitor ^{39}Ar production and establish neutron flux values (J) for the samples. Gas was extracted from samples via step-heating using a mid-infrared (10.6 μm) CO_2 laser with a non-gaussian, uniform energy profile and a 3.5 mm beam diameter rastered over a sample well. The samples were housed in a doubly-pumped ZnS-window laser cell and loaded into a copper planchette containing four square wells (1.6 cm^2). Liberated argon was purified of active gases, e.g., CO_2, H_2O, H_2, N_2, CH_4, using three Zr—Al getters; one at 16 °C and two at 400 °C. Data for 9 groundmass samples were collected on a GVi instruments ARGUS V multi-collector mass spectrometer using a variable sensitivity faraday collector array in static collection (non-peak hopping) mode (Sparks et al., 2008; Mark et al., 2009). Data for samples 10.2.15 and 11.1.15 were collected on a Mass Analyser Products MAP-215-50 single-collector mass spectrometer using an electron multiplier collector in dynamic collection (peak hopping) mode. Time-intensity data are regressed to inlet time with second-order polynomial fits to the data. The average total system blank for laser extractions, measured between each sample run, was $1.4 \pm 1.7 \times 10^{-15}$ mol ^{40}Ar, $2.8 \pm 3.5 \times 10^{-17}$ mol ^{39}Ar, $9.0 \pm 7.4 \times 10^{-18}$ mol ^{36}Ar ($2.75 \pm 0.09 \times 10^{-15}$, $3.0 \pm 0.5 \times 10^{-17}$ and $0.12 \pm 0.02 \times 10^{-18}$ respectively for samples 10.2.15 and 11.1.15). Mass discrimination was monitored on a daily basis, between and within sample runs by analysis of an air standard aliquot delivered by an automated pipette system (see raw data for D values applied to individual steps). All blank, interference and mass discrimination calculations were performed with the MassSpec software package (MassSpec, version 8.058, authored by Al Deino, Berkeley Geochronology Center). Inverse-variance-weighted plateau ages, or composite plateau ages for replicated samples, are chosen as the best estimates of the emplacement ages. Plateau ages were defined following these criteria:

1) Steps overlap in age within 2σ uncertainty.
2) Minimum ^{39}Ar content for a step is ≥0.1% of total ^{39}Ar release.
3) Minimum of three contiguous steps.
4) Minimum of 50% of ^{39}Ar in the chosen steps.
5) The inverse isochron formed by the plateau steps yields an age indistinguishable from the plateau age at 2σ uncertainty.
6) The trapped component composition, derived from this inverse isochron, is indistinguishable from the composition of air at the 2σ uncertainty level.
7) Age and uncertainty were calculated using the mean weighted by the inverse variance of each step.

Sanidine sample irradiation followed the same procedure as groundmass samples. Step-heated gas extraction used a narrower CO_2 laser beam with a 1.5 mm diameter. The samples were housed in a doubly-pumped ZnS-window laser cell and loaded into a stainless steel planchette containing 208 2.0 mm diameter round wells. Data were collected on a Mass Analyser Products MAP-215-50 single-collector mass spectrometer using an electron multiplier collector in dynamic collection (peak hopping) mode. The average total system blank for laser extractions, measured between each sample run, was $9.4 \pm 0.4 \times 10^{-16}$ mol ^{40}Ar, $9.6 \pm 2.6 \times 10^{-18}$ mol ^{39}Ar, $7.3 \pm 2.0 \times 10^{-18}$ mol ^{36}Ar. Other aspects of analysis were identical to those of the groundmass samples. Ages are presented at 2σ including uncertainty in J; uncertainties with and without J are presented in Supplementary material A.

Fig. 3. (previous page): Field photographs of aspects of the volcanic stratigraphy from both the Syunik and Vardenis volcanic highlands. (a) The summit area of Tskhouk polygenetic volcano in Syunik, showing a part of the caldera rim. (b) Sherepasar monogenetic volcano on the flank of Tskhouk, Syunik. The broad grassy ridge is formed by lava flows from the Tskhouk central volcano (P), while the monogenetic Sherepesar (M) is seen to overly these lava flows. Both Sherepasar and a sample from the Tskhouk lava flows were selected for dating. (c) Shows the ignimbrite at the base of the Vardenis volcanic succession capped by a lava flow. This ignimbrite was selected for $^{40}Ar/^{39}Ar$ dating. (d) Shows one part of the Karkar lava flow field which contains the youngest Holocene volcanoes in Syunik, including Paytasar shown in this photograph. Two distinct lava flows can be seen- one from Paytasar, and another probably younger lava flow from Nazelli volcano in front of it. In the background a sense of the scale of Karkar is apparant. (e) Torgomayr volcano in Vardenis. The ridges which form the flank of the volcano are formed by dacite lava flows, while the summit is a cap of basaltic trachyandesite (Sugden et al., 2019). The mafic cap was selected for $^{40}Ar/^{39}Ar$ dating. (f) Aerial photograph of Vayotsar scoria cone in the Vardenis highlands, showing the dimensions of its basal diameter and height. (g) Aerial photograph of Porak, a Holocene volcano in Vardenis, considered to be one of the youngest in the region. Here it is shown surrounded by lava flow fields.

5. New $^{40}Ar/^{39}Ar$ ages

The full Ar isotope dataset is displayed in Supplementary material A. A summary of these data is shown in Table 2, with examples of the associated isochron, step-heating plateau and population distribution (in the case of the sanidine phenocrysts) diagrams shown in Figs. 4 and 5. The full set of isochron and step-heating diagrams are shown in Supplementary material A. Fig. 4 shows the results of total fusion analyses of individual sanidine phenocrysts from an ignimbrite which forms the basement of the Southern Lesser Caucasus volcanic field in the Vardenis highland. Its age of 6.014 ± 0.067 Ma provides a maximum time frame over which most of the remainder of the southern Lesser Caucasus volcanic field was built. The late Miocene age correlates with a second pulse of post-collisional rhyolite volcanism across Armenia (7.5–4.5 Ma), with an earlier one occurring from 17 to 10 Ma (Karapetian et al., 2001). It also correlates with the end of the early stage of bimodal volcanism on the Erzurum-Kars plateau in neighbouring eastern Anatolia to the west, which included the production of felsic pyroclastic rocks (Keskin et al., 1998). This ignimbrite may have been part of a regional pulse of explosive felsic volcanic activity at this time.

All the other new ages (Fig. 5) are less than 1.5 Ma, as reported in Table 2. This is in agreement with other previous age constraints (Joannin et al., 2010; Ollivier et al., 2010; Lebedev et al., 2013), which suggest that the surface exposure of lava flows and un-eroded scoria cones in the Southern Lesser Caucasus volcanic field largely represents a Quaternary pulse in volcanism.

Sample 6–3-15 (Table 2) is from the small mafic dome which overlies the massive trachydacite units (Fig. 3e) and has a plateau age of 1.301 ± 0.014 Ma. This is 2.4 Myr younger than the dacites underneath. Such a time gap is greater than the range of ages for erupted products from the modern Aragats volcanic edifice (1.3 Myr; Connor et al., 2011; Gevorgyan et al., 2018, 2020), and the lifespan of Neo-Sabalan volcano in NW Iran (0.4 Myr; Ghalamghash et al., 2016). As such, this mafic unit is considered a separate monogenetic volcano from the dacites underneath.

In contrast, the age of the lava flow on Tskhouk polygenetic volcano (sample 5.5.12, Table 2) in Syunik is 1.316 ± 0.014 Ma, providing the first direct geochronological evidence that polygenetic volcanoes were active in Syunik within the past 1.5 Ma. All nine of the monogenetic volcano ages in Syunik are younger than 1 Ma (Table 2; Figs. 2 and 6). Fig. 6 shows the radiometric ages presented in this, and several previous studies (Karapetian et al., 2001; Joannin et al., 2010; Ollivier et al., 2010; Meliksetian et al., 2020). The spread of ages for monogenetic volcanism suggests that there may have been some pulses in activity, with more ages for the periods 1–0.8 Ma (9 ages) and 0.2–0 Ma (11 ages) than for the 600 ka in between (7 ages). However, given there are ~160 monogenetic centers in Syunik, significantly more than 27 ages will be required to properly elucidate the episodic history of volcanism in the region. Of the new ages presented here, 4 fall into the early "intense" period, 3 into the middle "quiet" period, and 2 into the most recent "intense" period. The most recent of these new ages is 0.048 ± 0.024 Ma (sample 11.3.15), although $^{40}Ar/^{39}Ar$ ages from the youngest Karkar lava flow field are as young as 9 ± 4 ka (Meliksetian et al., 2020). Fig. 6 shows that the mafic-intermediate monogenetic centers show some spatio-temporal coupling, with what appears to be a north-westward migration of vents with time. The correlation coefficient, r is −0.75 and 0.72 for latitude and longitude, respectively. It is certainly the case that volcanoes which are close together often have similar ages (Fig. 6).

The rhyolite obsidian sample (4.15.08) has an age of 0.672 ± 0.009 Ma, in good agreement with an apatite fission track age of 0.61 Ma (Karapetian et al., 2001). This could be part of a pulse in rhyolite volcanism across the Southern Lesser Caucasus volcanic field (including the Gegham highland to the north), with 11 ages for rhyolites in the 0.8–0.45 Ma range (there are 8 dated rhyolites which fall outside of this range; Karapetian et al., 2001; Lebedev et al., 2013).

Table 2
$^{40}Ar/^{39}Ar$ age determinations. Sample 4.15.08 is obsidian glass, 5.1.15 is sanidine phenocrysts, while all other samples are groundmass separates. For those samples that had their step heating experiments repeated, the age reported in the figures is the inverse-variance-weighted composite age highlighted in bold. Errors include J parameter. MSWD = mean square weighted deviation. Sample location co-ordinates can be found in the Summary Table in Supplementary Material A.

Sample cone/ lava/ tuff	Volcano (composition)	No. of steps	$^{40}Ar/^{39}Ar$ total gas age (ka)	$^{40}Ar/^{39}Ar$ weighted mean plateau age				$^{40}Ar/^{39}Ar$ isochron age			
				Age (ka) ± 2σ	%^{39}Ar	No. of steps in plateau	MSWD	Age (ka) ± 2σ	No. of steps in isochron	MSWD	$^{40}Ar/^{36}Ar$ (atm)
2.7.08 cone	Yerakov Blur (mafic)	16	887	894 ± 14	99	14	0.8	896 ± 16	14	0.85	298.5 ± 0.2
		15	883	892 ± 15	100	15	1.0	901 ± 18	15	0.86	298.4 ± 0.2
		29	895	**893 ± 12**	100	29	0.9	898 ± 14	29	0.83	298.5 ± 0.1
2.10.08 cone	Barurtumb (mafic)	14	886	878 ± 25	81.4	11	1.0	913 ± 71	11	1.02	289.6 ± 17.2
		14	857	853 ± 18	80.7	11	1.3	878 ± 36	11	1.09	289.9 ± 10.8
		22	861	**861 ± 15**	100	22	1.2	878 ± 34	22	1.21	293.4 ± 9.4
4.15.08 cone	Mets Satanakar (felsic)	15	685	674 ± 10	94.5	11	1.3	807 ± 322	11	1.37	288.4 ± 30.2
		15	669	670 ± 10	99.4	13	1.5	780 ± 221	13	1.56	290.5 ± 19.3
		24	672	**672 ± 9**	100	24	1.4	780 ± 140	24	1.34	290.5 ± 12
5.5.12 lava	Tskhouk (intermediate)	15	1303	**1316 ± 14**	89.6	8	1.2	1311 ± 20	8	1.27	302.5 ± 11
6.3.15 lava	Torgomayr (mafic)	15	1299	**1301 ± 14**	100	15	1.0	1307 ± 32	15	0.84	293.3 ± 5.8
8.3.15 cone	Verjiblur (mafic)	16	937	**957 ± 12**	89.1	9	1.0	973 ± 48	9	1.84	293.7 ± 14.2
9.1.15 lava	Spiovblur (mafic)	15	761	**817 ± 11**	81.7	9	1.1	820 ± 21	9	1.20	293.7 ± 14.2
9.2.15 cone	Chobanasar (mafic)	16	561	**571 ± 12**	100	16	1.5	569 ± 23	16	1.59	299.4 ± 6.9
10.2.15 lava	Kyorpasar (mafic)	15	147	164 ± 6	75.9	8	1.5	173 ± 11	8	1.06	292 ± 6.4
		15	140	175 ± 10	86.1	13	1.6	157 ± 22	13	1.45	304.6 ± 7.1
		21	154	**167 ± 5**	100	21	1.6	164 ± 11	21	1.68	300.3 ± 5.2
11.1.15 lava	Veckesar	15	348	**370 ± 8**	93.7	12	1.0	383 ± 11	13	0.75	296 ± 1.3
11.3.15 cone	Sherepasar (mafic)	13	40	42 ± 24	100	13	0.8	57 ± 34	13	0.81	297.7 ± 3.9
		17	67	55 ± 25	100	17	1.0	26 ± 13	17	1.01	300.4 ± 3.7
		30	57	**48 ± 18**	100	30	0.9	41 ± 15	30	0.92	299.0 ± 2.7
Single grain population age		No. grain				No. of grains for age			No. of grains for isochron		
5.1.15 tuff	Geghakar (Subatan) ignimbrite (felsic)	50		**6014 ± 67**		43	1.3	6017 ± 30	43	1.34	294 ± 32

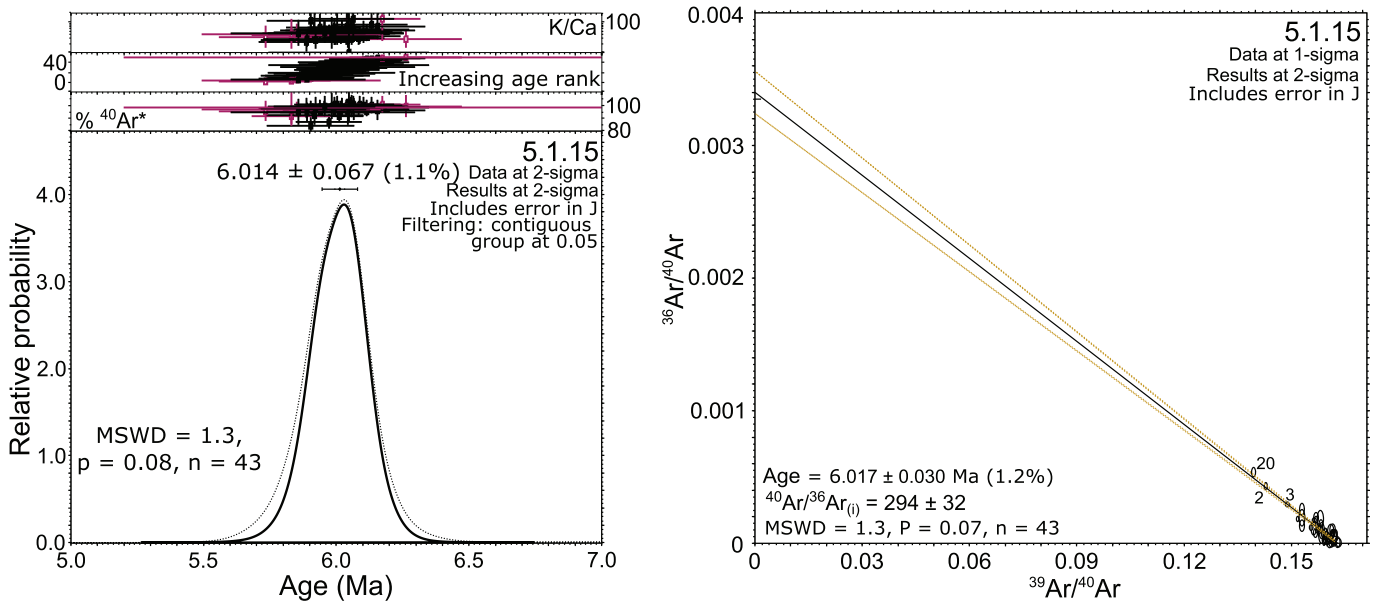

Fig. 4. Population distribution and inverse isochron diagram for ignimbrite sample from the base of the Vardenis volcanic highland. Symbols in red indicated rejected points. (For interpretation of the references to colour in this figure legend, the reader is referred to the web version of this article.)

6. Origin of the transition from polygenetic to monogenetic volcanism

The new $^{40}Ar/^{39}Ar$ ages obtained in this study support a temporal shift from polygenetic to monogenetic volcanism in Syunik. The age of the Tskhouk lava (1.316 ± 0.014 Ma- sample 5.5.12; Table 2) suggests the volcano could have still been active when the tephra layers were deposited in the diatomite sediments (1.24 ± 0.03 and 1.16 ± 0.02 Ma; Section 2.1). These tephra layers could then be sourced from local Plinian eruptions, and may in fact be the youngest marker of polygenetic volcanism in Syunik. After 1 Ma the polygenetic edifices were covered by younger monogenetic volcanoes and their associated lava flow fields (Fig. 7). These lava flows were predominantly mafic-intermediate in composition, except for a small area in the north of Syunik which includes rhyolite domes and flows (Figs. 2 and 7).

The age of the mafic scoria from the summit of Torgomayr volcano (Fig. 3e; sample 6.3.15) of 1.301 ± 0.014 Ma (Table 2) supports the interpretation that by this time (1.5–1 Ma), Vardenis was already a region of monogenetic volcanism, while volcanoes in Syunik were still polygenetic. Unfortunately, the old age of the ignimbrite (Fig. 4; Table 2- sample 5.1.15) at 6.014 ± 0.067 Ma does not provide much further constraint on how recently volcanism was polygenetic.

The question then arises: did volcanism in Syunik around 1 Ma transition from polygenetic to monogenetic due to a decreasing magma supply, increasing rates of crustal extension or both? These possibilities and their implications are now discussed.

6.1. A low rate of magma supply?

One way to look at the rate of magma supply is to investigate the recurrence rate of volcanic eruptions. If a constant repose interval is assumed this can be written as:

$$\lambda_t = \frac{N-1}{t_0 - t_y} \quad (1)$$

If it is assumed that each eruption forms a new vent, then we can take the number of eruptions (N) as being the number of monogenetic vents present in Syunik (160). The oldest age for a lava sample from one of the monogenetic volcanoes is 0.993 Ma (one of the lava flows capping the Sisian suite diatomite sediments; Fig. 2; Ollivier et al., 2010), which is taken as the value for t_0 (Fig. 6). The youngest eruption (t_y) is taken as 0.009 Ma on the basis of $^{40}Ar/^{39}Ar$ ages from the Karkar lava flow field (Meliksetian et al., 2020). This calculation results in 1.6×10^{-4} eruptions/year, within the range of volcanic fields globally (10^{-4} to 10^{-5} eruptions/year; Connor and Conway, 2000). When the areal extent of different volcanic fields is considered, Syunik is towards the upper limit of spatio-temporal eruption frequency for volcanic fields globally (Table 3).

This is consistent with the presence of andesite and rhyolite monogenetic volcanic centres in Syunik. The Sr—Nd isotope systematics of volcanic rocks from Syunik show that the evolved magma compositions are not the result of crustal melting or assimilation (Sugden et al., 2019). The production of evolved magmas requires a thermal anomaly in the crust substantial enough to allow magmas to stall and fractionate while retaining a sufficient melt fraction to remain "eruptible" (Sparks et al., 2019). As such, evolved compositions are thought to be associated with volcanic fields with a relatively high rate of magma supply (Smith and Németh, 2017). If the eruptive flux was higher in the past (perhaps by an order of magnitude- Table 3), this could have been sufficient for volcanism to have formed polygenetic volcanoes.

If volcanic activity is waning in the Lesser Caucasus, we would expect to see a decrease in magmatic output over the course of the last 1 Ma of monogenetic activity in Syunik. One way of looking at this is to consider whether there has been a decrease in eruption frequency with time. This approach assumes that the average volume of eruptions remains static over the period. Here, we have only the limited dataset provided by radiometric ages from this study and elsewhere in the literature (30 ages vs. 160 mapped vents). Only monogenetic volcanism is considered here, due to the paucity of ages for the eruptions of the local polygenetic volcanoes. The rate of volcanic eruptions in Syunik appears to be highest for the periods of 1–0.8 Ma and 0.2–0 Ma (Fig. 8). To a first order, the age distribution does not appear to show waning volcanic activity. At the 95% confidence interval, the Syunik ages are indistinguishable from a steady-state model (Fig. 8).

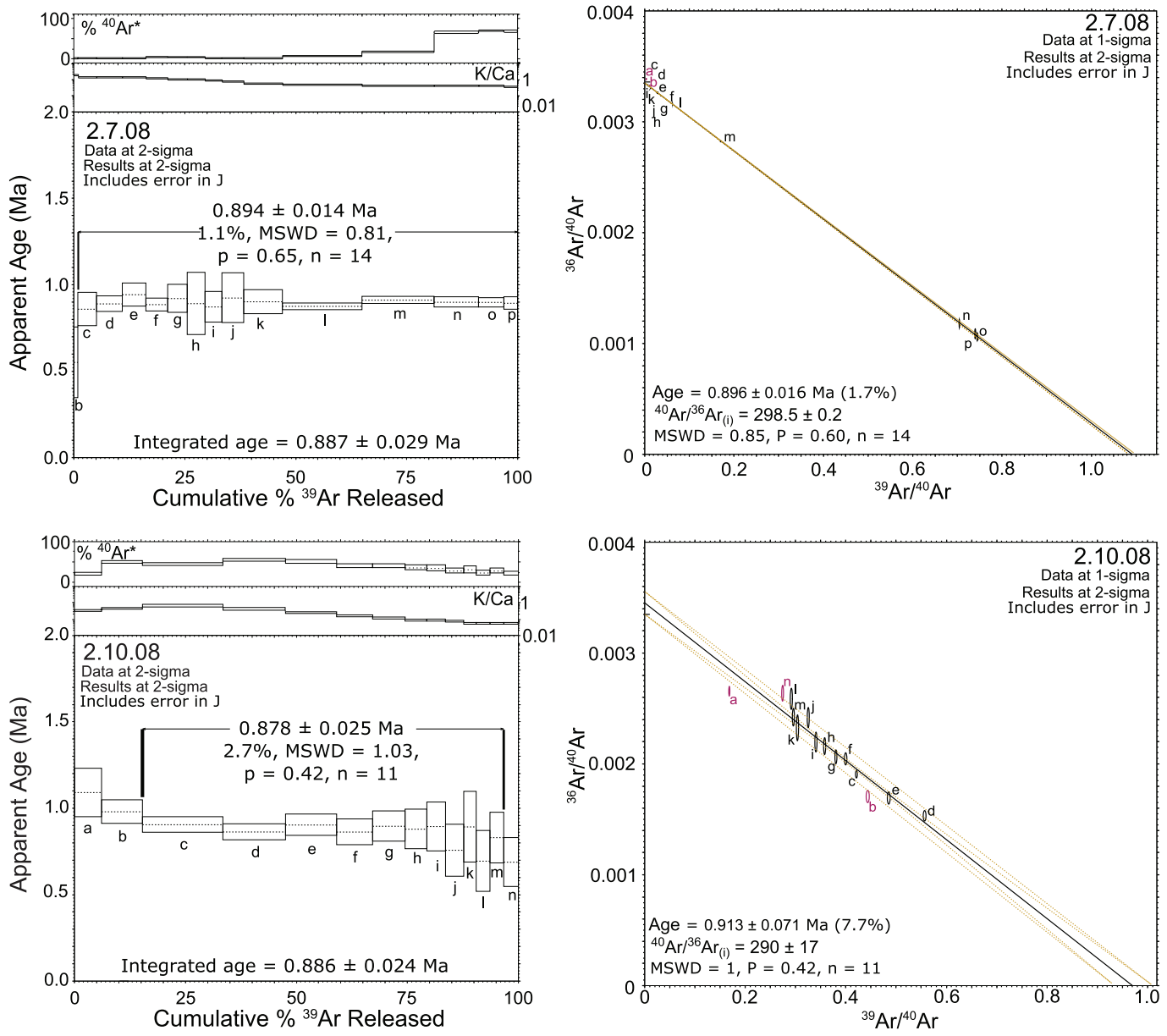

Fig. 5. Two examples of plateau and isochron diagrams for $^{40}Ar/^{39}Ar$ step-heating experiments on groundmass samples. Symbols in red indicate rejected points. (For interpretation of the references to colour in this figure legend, the reader is referred to the web version of this article.)

It is possible that with more ages, volcanism could be shown to deviate from steady-state. This is illustrated in Fig. 8, with a comparison to ages ($n = 43$) from the nearby Gegham volcanic highland (ages from Lebedev et al., 2013). The extra ages in Gegham show that the pulses of volcanic activity seen there do not fit a steady-state model. An alternative approach to predict the effect of more ages on the Syunik age distribution is to look at the volcano stratigraphy. Where volcanoes lie directly above or below volcanic units which have been age-constrained, maximum and minimum ages can be assigned to these volcanoes. This is shown for Syunik in Table B.1 (Supplementary material B). Where a maximum age is not available, the upper limit is assumed to be 1 Ma based on the range of ages observed for monogenetic volcanoes in Syunik. If the ages of these volcanoes are taken as the mid-point between the maxima and minima, they do not have a significant effect on the age distribution, with volcanism still appearing to be steady state (Fig. 9).

For Syunik, the 1–0.2 Ma period does show diminishing volcanic activity- albeit not to a sufficient degree to allow it to be definitively distinguished from a steady state model. During this period there are pulses of volcanic activity at different times in Gegham and Syunik, but both show a sharp increase in ages after 0.2 Ma (Fig. 8). This latter feature could reflect a sampling bias. Older vents are more likely to be buried by subsequent eruptions. Volcanologists will often target the youngest vents for dating as they provide important information with regard to the local volcanic hazard. The youngest lava flows are also likely to provide the best quality samples for geochemical analysis. If the apparent pulse after 0.2 Ma is the result of sampling bias and can be ignored, then perhaps the evidence from 1 to 0.2 Ma (Fig. 8) does show the rate of volcanic eruptions in Syunik is waning.

Another possibility is that the frequency of eruptions is indeed stead-state, but this frequency might not reflect the change in magma supply with time. It is possible that the volume of eruptive events has

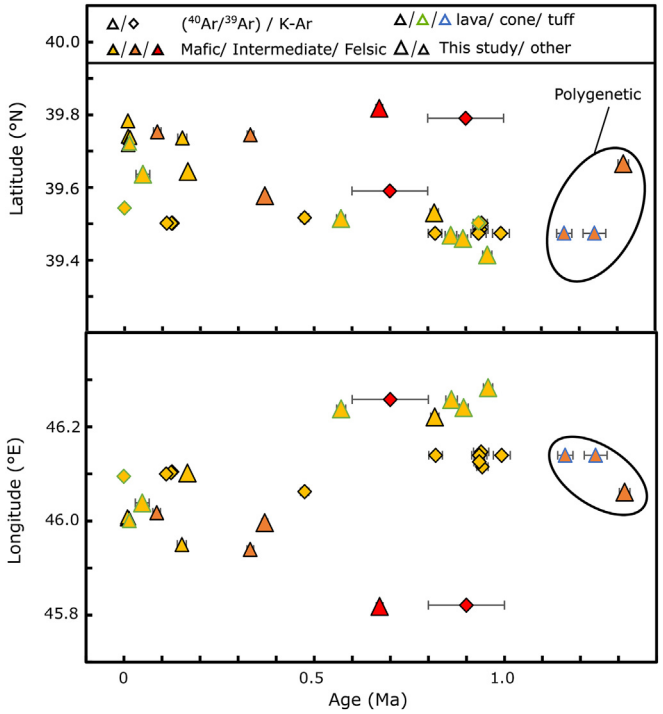

Fig. 6. The ages of radiometrically dated samples from both this study and others vs the latitude and longitude of the sample. Error bars represent 2σ uncertainties. The shape of the symbol denotes the method of dating- triangles for $^{40}Ar/^{39}Ar$, diamonds for K—Ar. The area circled as polygenetic shows the ages thought to be associated with eruptions of a polygenetic volcano. The large triangle is the age of the lava from Tskhouk dated for this study. The two smaller triangles are pumice layers in diatomite sediments (Joannin et al., 2010). For the mafic-intermediate monogenetic volcanoes, the correlation coefficient with age is −0.75 and 0.72 for latitude and longitude, respectively. Literature ages are from Karapetian et al. (2001); Joannin et al. (2010); Ollivier et al. (2010) and Meliksetian et al. (2020).

decreased over time. The volume of the Karkar lava flow field can be taken as an estimate of the erupted lava volume during the Holocene in Syunik (Fig. 2). Karkar can be compared with an estimate for the volume of lava erupted from monogenetic vents since 1 Ma.

The volume of the Karkar lava flow field has been estimated as 0.3 km^3, assuming an average thickness of ~10 m for lava flows (Meliksetian et al., 2020). If this value is taken as the total erupted volume for the last 15 ka, this would give a magma output rate of 2×10^{-5} km^3yr^{-1}.

The mapped area of lavas from monogenetic vents in Syunik (Fig. 2) is 680 km^2. This figure includes mafic-intermediate and rhyolite monogenetic volcanoes, as well as the Holocene lava flows. Several monogenetic volcanoes are buried by glacial drift (Fig. 2), such that the area (and thus volume) calculated is likely to be a slight underestimate. The estimate for the thickness of monogenetic lavas is based on sections across the Shamb gorge reported in Ollivier et al. (2010), as well as borehole data from close to the Karkar lava flow field (Gilliland et al., 2018). In the Shamb gorge, lacustrine sediments from the Sisian suite are capped by lava flows, the latter of which are all younger than 1 Ma. Due to their age, the lava flows are interpreted as monogenetic. The lava flow cap is between 100 m and 500 m thick. The high end of this thickness range will represent several generations of lava flows. For example, the 500 m thick section is a succession of 4 lava flows that are 60–170 m thick (Ollivier et al., 2010). This thickness estimate is supported by boreholes drilled close to the Karkar lava flow field (Fig. 2), which show the post-collisional lavas to be ~700 m thick (Gilliland et al., 2018). Again, this thickness will represent several generations of lava flows; the thickness of some of the individual lava flows which have been dated is shown in Table 4. Some of the lavas towards the base of this section could represent eruptions from the nearby Tskhouk polygenetic volcano, and therefore this 700 m thickness is an upper limit on the thickness of monogenetic deposits. For a lower limit on lava flow thickness, 100 m is considered unrealistic given that: (i) the Shamb gorge is on the edge of the volcanic area and deposits are likely to be thicker in the interior; (ii) single lava flows have thicknesses of up to 110 m (Table 4); and (iii) in some cases there are clearly multiple generations of monogenetic lavas- including in the Shamb gorge and where Holocene lava flows cover older monogenetic vents (Meliksetian et al., 2020). We use a thickness range of 300–700 m for the monogenetic lava flow sequence to estimate the volume of lava produced by monogenetic eruptions in Syunik as between 204 and 475 km^3, equivalent to a magma output rate of between 2×10^{-4} and 4.8×10^{-4} km^3yr^{-1}. These are uncorrected values, and do not represent dense rock equivalents (where factors including vesicularity and surface roughness are factored in). The resulting overestimation in our calculation is likely to be minor relative to the uncertainties in the thickness estimate.

The Holocene magma output rate is lower than the overall rate for the last 1 Ma, by around an order of magnitude. This suggests a decreasing magma output rate with time. Given that the recurrence rate of volcanic activity is at the high end of eruption rates for monogenetic volcanic fields (Table 3), it is plausible that a higher magma supply in the past led to the construction of polygenetic volcanic edifices. However, it should be noted that the volume estimate for the Karkar lava flow field represents a snapshot of just the last 15 ka of activity- or ~ 1.5% of the lifetime of monogenetic volcanism in Syunik. Given the evidence that volcanic activity could potentially occur in pulses (Fig. 8), further evidence for a decreasing magmatic output from eruptions in the region is needed.

A point worthy of note here is that Syunik has the highest density of monogenetic volcanic centers (0.071 per km^2) in the Lesser Caucasus (Fig. 10). The spatial density map in Fig. 10 is calculated for a 10×10 km grid and is based on a Gaussian kernel function, with the contours representing the likelihood that the next eruption will form a vent within a 10×10 km grid area at that location (see Fig. 10 caption for details). The Syunik maximum (a spatial intensity of 0.15 vents/km^2 for the 0.05 contour in Fig. 10) may indicate the highest local magma flux in the region. Syunik was also host to polygenetic volcanism more recently than some of the other regions to the north. If magma supply has been decreasing across the region, then volcanism may have shifted from polygenetic to monogenetic last of all in Syunik, where the long-term eruption rate is highest.

The volcanic structures in the Lesser Caucasus may well suggest a decreasing rate of magma supply across the region. Volcanism between 3.25 and 2.05 Ma produced 200-400 m thick flood basalts, which have been proposed as the youngest continental flood basalt province in the world (Sheth et al., 2015). The subsequent period then seems to be characterized by the construction of large volcanoes capable of erupting large volumes in single events, but with eruptions perhaps more intermittent and of a more intermediate composition than during the first phase. For example, the ages of ignimbrites from Aragats volcano range from 1.8 to 0.65 Ma (Ghukasyan, 1985; Mitchell and Westaway, 1999; Chernyshev et al., 2002; IAEA-TECDOC-1795, 2016; Gevorgyan et al., 2020), while eruptions of Tskhouk and/or Ishkhanasar volcanoes occurred until ~1 Ma. The most recent eruptions appear to have derived exclusively from small monogenetic eruptive centers in NW Armenia, Gegham, Vardenis and Syunik (Karakhanian et al., 2002; Lebedev et al., 2013; Neill et al., 2013). This history corresponds with the Valley, Ridge and Cone series of Neill et al. (2013). To summarise, the volcanic stratigraphy suggests there has been a decreasing rate of magma supply across the Lesser Caucasus during the past ~3 Ma. A polygenetic to monogenetic transition in volcanic activity is most clearly seen in Syunik because it happened most recently there. This is likely to be the result of the Syunik highland having the highest magma flux, as evidenced by the highest density of volcanic centers being focused on Syunik (Fig. 10).

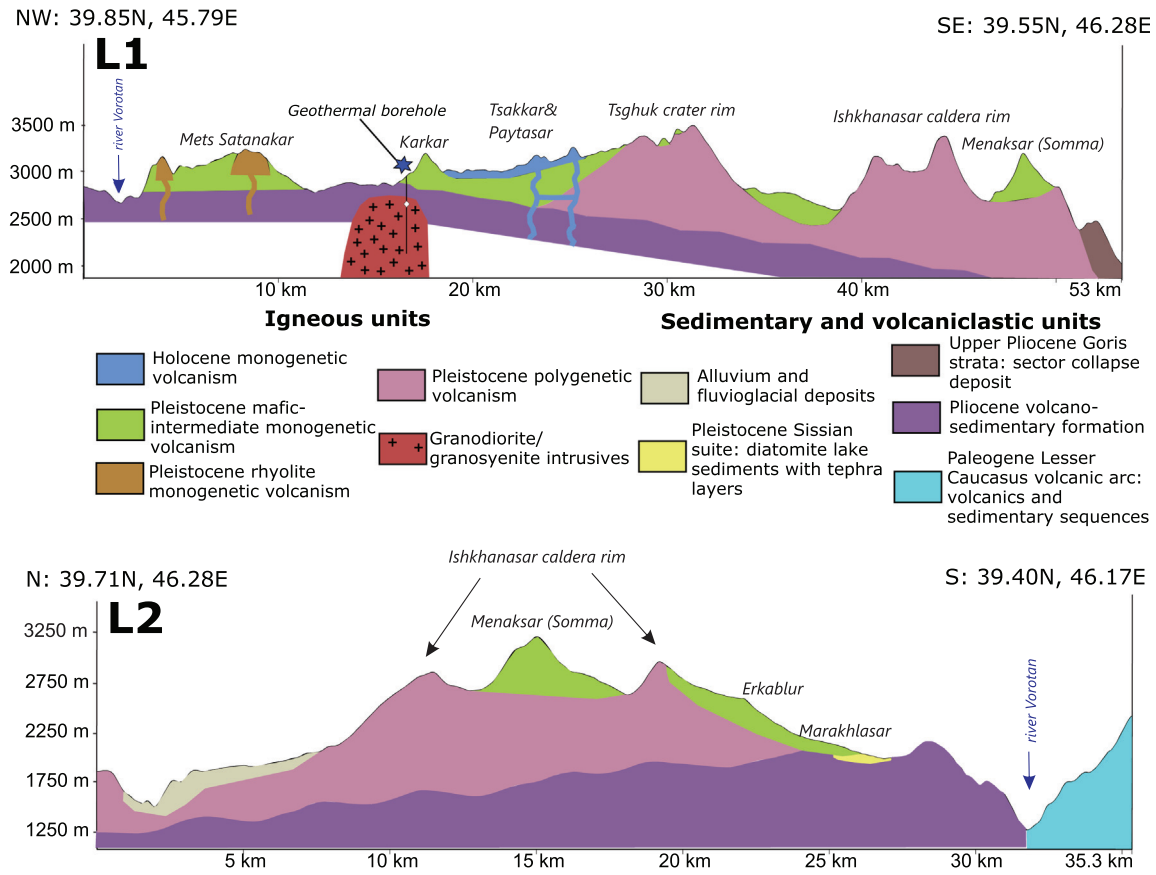

Fig. 7. Sketch cross sections of the Syunik volcanic highland. The lines of section L1 and L2 are shown in Fig. 2. Volcanism prior to 1 Ma was dominated by large polygenetic volcanoes, of which there were at least 2, possibly of multiple generations. Mafic-intermediate monogenetic volcanism younger than 1 Ma overlies the polygenetic volcanoes. Individual scoria cones may be associated with lava flow fields of variable sizes. Dykes, sills and conduits must have supplied these vents, and a couple of these are illustrated for the Holocene and rhyolite volcanism. Monogenetic felsic volcanism also occurred in the last 1 Myr, and was localised in the north of the Syunik volcanic highland (line L1). Without more borehole data, the deeper parts of the cross section are speculative. The intrusive unit which does not outcrop at the surface is shown on the basis of one of the three geothermal boreholes (Gilliland et al., 2018).

Table 3
The spatio-temporal frequency of volcanic eruptions from Syunik and other volcanic fields worldwide (after Connor and Conway, 2000).

Volcanic field	Area (km^2)	Eruptions per year	Eruptions/yr/km^2
Cima, CA, USA	150	0.00008	5.33×10^{-7}
Eifel, Germany	1000	0.0005	5.00×10^{-7}
Syunik, Armenia	**1100**	**0.00016**	**1.45×10^{-7}**
Klyuychevskoy, Kamchatka, Russia	2500	0.0002	8.00×10^{-8}
Springerville, AZ, USA	3000	0.0002	6.67×10^{-8}
Big Pine, CA, USA	500	0.00002	4.00×10^{-8}
Camargo, Mexico	2500	0.0001	4.00×10^{-8}
Coso, CA, USA	1200	0.00003	2.50×10^{-8}
San Francisco, AZ, USA	5000	0.0001	2.00×10^{-8}
Yucca Mt., NV, USA	1200	0.00001	8.33×10^{-9}
Trans-Mexican volcanic belt	40,000	0.0003	7.50×10^{-9}
Pancake, NV, USA	2500	0.00001	4.00×10^{-9}

The question then arises- why has this decrease in magma flux occurred? One option is that what we are seeing is the death of a subduction zone- that since the end of the supply of slab-derived components with continental collision, continued melting of the mantle source has exhausted it of fusible components, leading to reduced melt production. This should lead to a more depleted mantle source with time.

Bulk-rock major and trace element concentrations in lavas reflect the composition of the magma source, the degree of melting, and assimilation plus fractional crystallization processes. Elements such as Ca and Al might be expected to become depleted in a less enriched mantle source due to the exhaustion of clinopyroxene during progressive melt extraction. However, any such trends in element concentrations for the Armenian volcanic rocks are masked by the overprint of fractional crystallization, given that the lavas in Syunik represent a complete compositional range from basanite to rhyolite (Sugden et al., 2019). In a closed system, isotope ratios do not fractionate with progressing melting and crystallization and instead reflect the magma source rocks. As there is no evidence for crustal contamination (Sugden et al., 2019), the Sr-Nd-B isotope composition of magmas should reflect their mantle source. Therefore, one would expect to see lower $^{87}Sr/^{86}Sr$ and $\delta^{11}B$, and higher $^{143}Nd/^{144}Nd$ with time and mantle depletion. This is because the components of the mantle source derived from subduction will have higher $^{87}Sr/^{86}Sr$, lower $^{143}Nd/^{144}Nd$, and heavier $\delta^{11}B$ than those typical of the depleted mantle. As Fig. 11 shows, this trend is not seen for $\delta^{11}B$ and $^{143}Nd/^{144}Nd$, however some of the youngest samples do show lower $^{87}Sr/^{86}Sr$. One exception to this trend of lower $^{87}Sr/^{86}Sr$ is the lava from Porak, which has similar $^{87}Sr/^{86}Sr$ to the older samples (Fig. 11). All the samples with a lower $^{87}Sr/^{86}Sr$ outcrop within 12 km of each other, and as there is a north-eastward migration in vent location with time, the trend to lower $^{87}Sr/^{86}Sr$ could just as easily reflect small-scale mantle heterogeneity beneath the Syunik highland (Fig. 6).

Despite the suggestion that volcanism is waning, there is no direct evidence for the exhaustion of the subduction component in the mantle source. Waning volcanism could instead be related to a reduced volume of mantle involved in melting, or melt extraction processes giving an

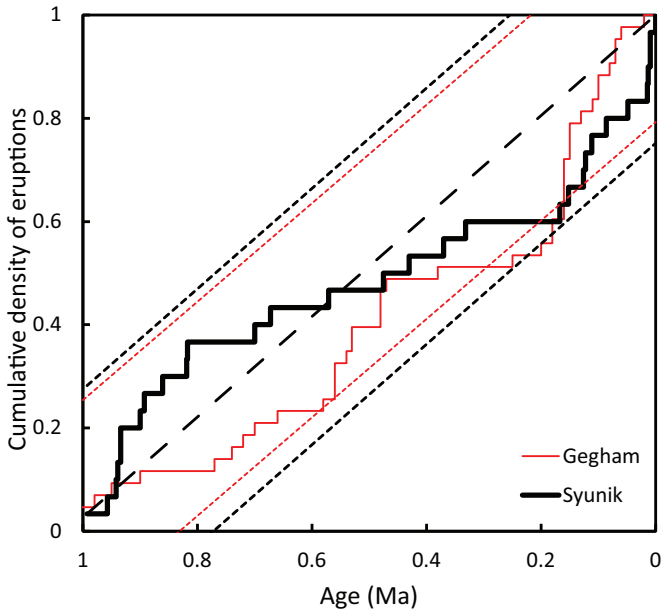

Fig. 8. Cumulative distribution function for ages of Pleistocene volcanic rocks monogenetic volcanoes. The age distribution of Syunik is shown by the bold black line. The dash-dot line shows the steady-state model, with the 95% confidence interval for the Syunik samples shown by the two dashed lines. The Syunik age distribution is contained entirely within this interval. K—Ar ages from the nearby Gegham volcanic highland (Fig. 1; Lebedev et al., 2013) are shown for comparison in red. The larger number of ages from Gegham compared to Syunik (43 vs 23) gives a narrower steady state confidence interval. The Gegham age distribution is outside the bounds of the steady-state model, meaning this age distribution is unlikely to represent steady-state volcanism. That Syunik is within the 95% confidence interval means that the volcanism there could potentially be steady state. Ages for Syunik are a mixture of K—Ar and $^{40}Ar/^{39}Ar$ ages as shown in Figs. 2 and 6. Data are from this study as well as Karapetian et al. (2001); Joannin et al. (2010); Ollivier et al. (2010); Meliksetian et al. (2020). (For interpretation of the references to colour in this figure legend, the reader is referred to the web version of this article.)

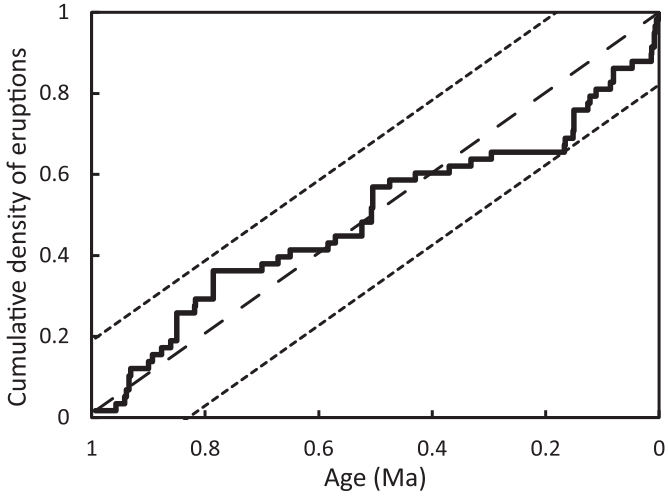

Fig. 9. Cumulative age distribution as in Fig. 8. Here, the additional age estimates from the stratigraphy are also included, taking the estimated ages column from Table B1 (Supplementary Material 2). The addition of stratigraphic age constraints does not substantially alter the age distribution, suggesting the assumption of steady-state volcanism (in terms of eruptions) could hold with more age constraints. However as discussed in the main text, it may be the case that the volume of volcanic eruptions decreases with time. As in Fig. 8, the dash-dot line represents the steady-state model with the dashed lines giving the 95% confidence range.

Table 4
The thickness of lava flows erupted from some of the volcanoes which have been radiometrically dated.

Volcano	Latitude (°N)	Longitude (°E)	Composition	Age (Ma)	Lava flow thickness (m)
Merkesar	39.58566	46.23778	Trachydacite	0.7	110
Chobanasar	39.52222	46.23833	Basanite	0.571	30
Veckesar	39.57705	45.99658	Trachybasaltic andesite	0.37	8
Kyorpasar	39.64401	46.10200	Trachybasaltic andesite	0.167	1–2
Sherepasar	39.64139	46.04000	Basanite	0.048	20

initial pulse of magma which decays away. Previous studies have argued that magma generation occurs in the lithosphere in response to heating (Neill et al., 2015; Sugden et al., 2019). An initial event, perhaps of small-scale delamination (or lithospheric dripping; Kaislaniemi et al., 2014) could be the trigger for this Plio-Pleistocene pulse in volcanism, which produced initially large volumes of magma that then decayed with time.

It is perhaps unsurprising that we see no evidence for exhaustion of the mantle source. Although geochemical studies of monogenetic volcanic fields commonly reveal evidence for mantle source heterogeneity (e.g. Hickey-Vargas et al., 2002; Arce et al., 2013), examples of a systematic temporal change in geochemistry associated with a polygenetic to monogenetic transition are rare. One exception comes from central America, where Quaternary monogenetic volcanoes in western El Salvador and southeastern Guatemala become systematically depleted in Cs/Zr, La/Zr and $\delta^{18}O$ with time (Walker et al., 2011). However, this trend was argued to be the result of decreasing crustal contamination, not a mantle source effect. Crustal contamination is not thought to play a significant part in the petrogenesis of Syunik lavas (Sugden et al., 2019). Those geochemical distinctions that can be observed in the Syunik volcanic highland are also likely to be associated with magma evolution in the crust. All of the polygenetic lavas sampled have intermediate compositions (trachyandesite), while the monogenetic lavas show a complete compositional range from basanite to rhyolite (Sugden et al., 2019). This might attest to the importance of mixing between mafic and felsic magmas in the plumbing systems of the polygenetic volcanoes. Our observation seems to support the theory that the prevalence of andesites in arcs results from magma mixing (Reubi and Blundy, 2009).

The continuous geochemical trend observed in central America was associated with a trenchward migration in volcanism that resulted from the westward movement of the locus of rifting. Older (lower Pleistocene) polygenetic volcanoes argue for a polygentic to monogenetic transition driven by increased crustal extension in that part of central America (Walker et al., 2011). The possibility that this has occurred in Syunik is the focus of the next section.

6.2. Increased extension rate?

Many of the youngest generation of volcanoes (Holocene) form small clusters which are located in modern pull-apart basins, including several of the youngest cones in the Gegham highland (labelled GM in Fig. 1; Sargsyan et al., 2018), at Porak in Vardenis (Karakhanian et al., 2002) and the Karkar group of lava flows and scoria cones in Syunik (Fig. 2). There is a degree of spatio-temporal coupling in Syunik, with vents located close together often having similar ages (Figs. 2 and 6). Clusters of vents with a similar age could therefore reflect previously active pull-apart basins. Although it has been suggested such clusters could form over enriched domains in a heterogeneous mantle (Valentine and Connor, 2015), the variation in $^{87}Sr/^{86}Sr$ (Fig. 11c) suggests magmatism tapped both enriched and depleted domains.

Extensional structures have clearly interacted with magmatism in the Lesser Caucasus. The question is then how could this extension relate to the polygenetic to monogenetic transition at 1 Ma in Syunik?

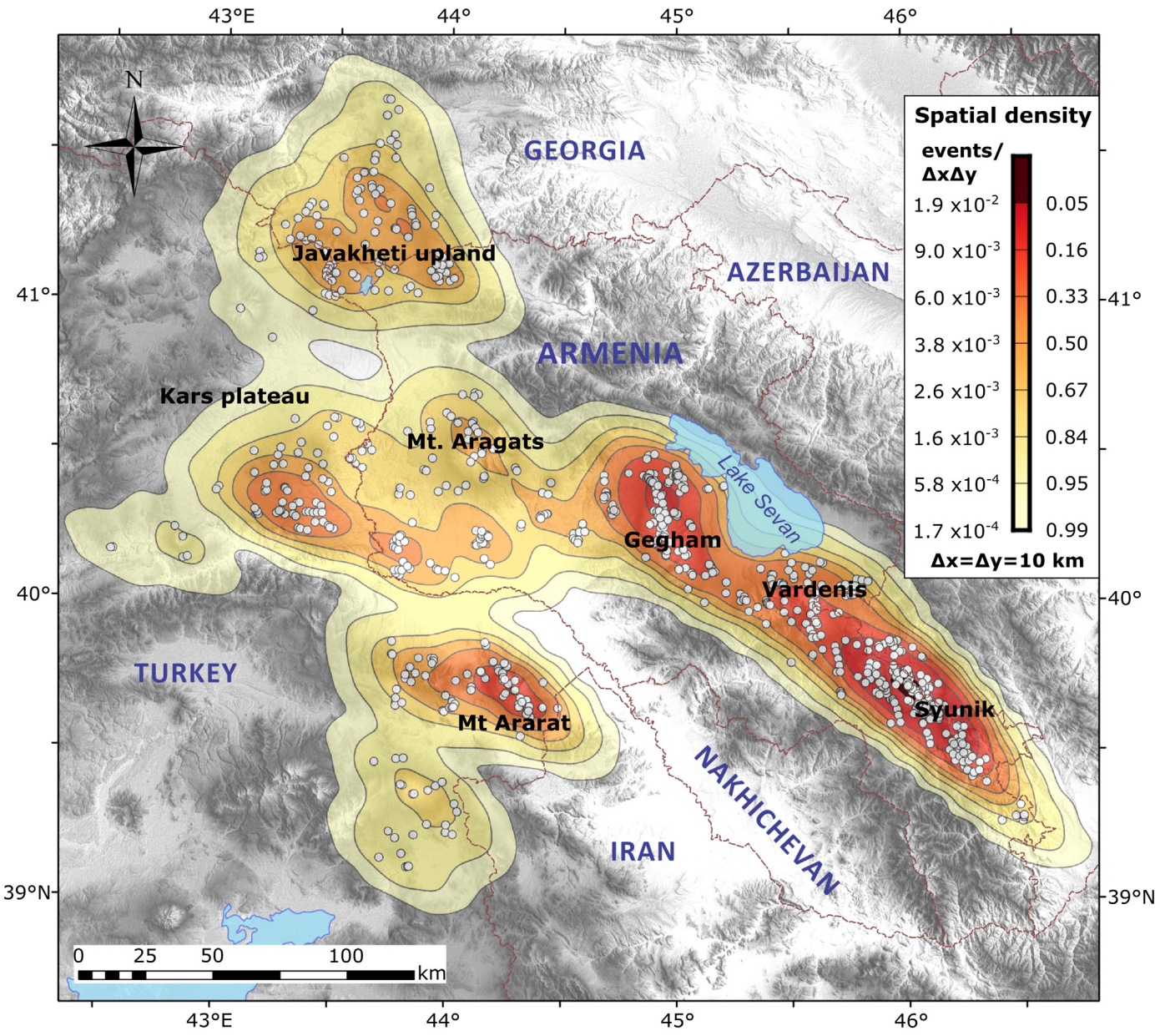

Fig. 10. Spatial density model of Quaternary volcanic centers in Lesser Caucasus region including Armenia, south-east Georgia, and eastern Turkey. Model is based on 772 volcanic centers from the database at the Laboratory of Volcanology, Institute of Geological Sciences, National Academy of Sciences of the Republic of Armenia. Remote sensing data by A. Karakhanyan. The spatial density contours are calculated in "perl" using the "ks" package (Duong and Hazelton, 2003) using a 10 × 10 km grid. The calculation can be considered analogous to a histogram. By using a large grid spacing, each histogram bin covers a larger area, and counts per bin are high, giving higher reported spatial density values. However, the grid spacing does not affect the shape of the mapped contours. The Gaussian kernel function was calculated using a SAMSE bandwidth (sum of asymptotic mean squared error). The contours plotted represent the distribution of vent density. The events/ΔxΔy values represent the probability of the next vent forming in a 10 × 10 km grid area around that location. Across the whole map these values will integrate to 1 (or close to), given there is a very high probability the next vent will form within the mapped area. Spatial intensity gives a closer approximation of cone density in a given region and can be calculated by multiplying the spatial density values by the total number of vents on the map (in this case 772). To understand the percentiles, taking the 0.33 contour, there is a 33% chance that the next eruption in the Lesser Caucasus will occur within the regions enclosed by that contour. For further details on generating a spatial density map, please refer to (Connor et al., 2019).

The most obvious model would be for the rate of deformation to have increased at that time. However, the rate of motion on the Pambak-Sevan-Syunik fault (PSSF, the major strike slip fault in the area) has been constant over the past 1.4 Myr at 1 mm/yr, at least on the southern branch close to the volcanoes in Syunik (Karakhanyan et al., 2013). This was established on the basis that modern fault creep measured using GPS is indistinguishable from a long-term average estimate for fault motion- estimated using the offset of a 1.4 Ma monogenetic cone which was cut by the fault (Philip et al., 2001; Karakhanyan et al., 2013). Hence, on the basis of strike-slip motion there is no evidence for increasing deformation rates across the time interval of the polygenetic to monogenetic transition.

During their lifetime faults increase in length. Field mapping suggests that Syunik is at the southern extremity of the modern PSSF, in which case the fault might not have been active in Syunik in the past. However, it is possible the fault zone extends southward in the subsurface (Karakhanyan et al., 2016), making it more likely to have been active locally during the transition. E Either way, there is no reason to believe that localised extension was necessarily lower in Syunik in the past, because there may have been other smaller fault systems

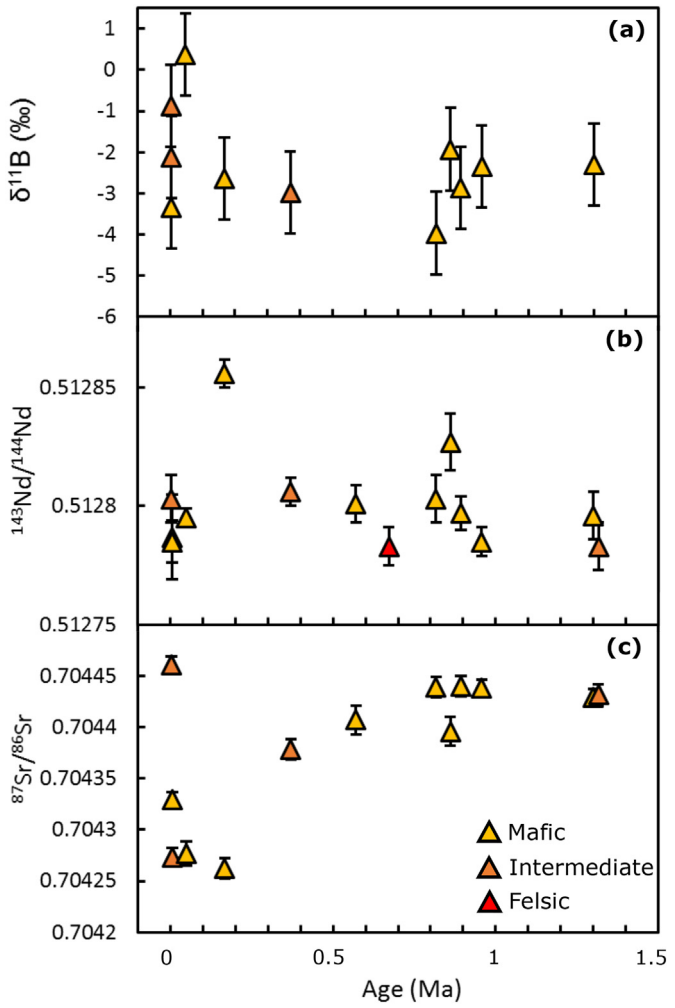

Fig. 11. $\delta^{11}B$, $^{143}Nd/^{144}Nd$ and $^{87}Sr/^{86}Sr$ vs age. The isotope data is from Sugden et al. (2019) and Sugden et al. (2020). While $\delta^{11}B$ (a) and $^{143}Nd/^{144}Nd$ (b) show no correlation with age, some of the younger samples have lower $^{87}Sr/^{86}Sr$ (c). Error bars for $\delta^{11}B$ are given as 1‰, on the basis of the reproducibility from duplicate analyses (Sugden et al., 2020). Error bars for $^{143}Nd/^{144}Nd$ and $^{87}Sr/^{86}Sr$ are 2σ analytical uncertainties.

accommodating extension, as is currently seen in the Gegham volcanic highland (Fig. 1).

Some monogenetic volcanoes appear to be unrelated to local extensional structures. The cones of the Shamiram plateau on the southern flank of Aragats volcano show no preferred alignments, and likely formed in the absence of any local normal faults (Connor et al., 2011). Two of the youngest volcanoes in the Vardenis highland - Vayotsar (Fig. 3f) and Smbattasar- both formed in isolation and away from the pull-apart structures hosting Porak volcano. Local normal faults may well provide a favourable pathway for ascending magmas, but they do not appear to be required for monogenetic volcanism in the Lesser Caucasus. That said, the presence of an extensional component in regional deformation (Karakhanyan et al., 2013) could have promoted the development of monogenetic volcanism, as has been suggested in other settings (Takada, 1994a; Bucchi et al., 2015). However, the lack of evidence for an increase in the rate of crustal extension during the Pleistocene suggests that it was not the driving force for the polygenetic to monogenetic transition.

6.3. Southern Lesser Caucasus volcanism within the context of global polygenetic and monogenetic activity

Terrestrial volcanic activity is a continuum between truly polygenetic and monogenetic activity. Many volcanic complexes around the world can be considered intermediaries between the two end-members: Ceboruco in Mexico with its numerous parasitic cones (Sieron et al., 2019b), the collection of small polygenetic volcanoes of the Kirishima complex in southern Japan (Nagaoka and Okuno, 2011), and the multitude of vents that have been mapped on the Lassen Peak complex, California (Germa et al., 2019). We see this same continuum in the Syunik and Vardenis highlands. Polygenetic volcanism is exemplified by Tskhouk (Fig. 3a) and Ishkhanasar volcanoes, as well as the basal ignimbrite in Vardenis (Fig. 3c) which is likely to have formed from a caldera-collapse eruption. At the other end of the spectrum is Vayotsar volcano in Vardenis, which formed in isolation in a single eruptive event (Fig. 3f). In between we have complexes like Karkar (Fig. 3e) and Porak (Fig. 3g), where closely spaced monogenetic vents effectively build small volcanic complexes.

There are several studies that have looked at a polygenetic to monogenetic transition. In some localities, such as the Higashi-Izu region of Japan (Hasebe et al., 2001), and back-arc volcanism in south-east Guatemala and western El Salvador (Walker et al., 2011), a change in the local stress field brought on by a tectonic re-organisation is implicated in the transition. In another case, Bucchi et al. (2015) investigated the close proximity of the Carrán–Los Venados volcanic field (monogenetic) and the Puyehue–Cordón Caulle volcanic complex (polygenetic) in the southern Andes. They argued volcanism was monogenetic at Carrán–Los Venados because of both a higher extension rate and lower magma supply. The Syunik volcanic highland is an important case study of a polygenetic to monogenetic transition driven predominantly by a decreasing magma supply, without any change in the local stress field.

7. Conclusions

All but one of the new $^{40}Ar/^{39}Ar$ ages from the southern Lesser Caucasus are younger than 1.5 Ma, suggesting that the bulk of exposed post-collisional volcanic rocks are from mid- to late Pleistocene eruptions. However, the ignimbrite age of 6 Ma shows the region has been host to post-collisional volcanism since at least the late Miocene. The new ages confirm that a transition from polygenetic to monogenetic volcanism occurred around 1 Ma in the Syunik highland, while in the Vardenis highland to the north volcanism was already monogenetic by 1.4 Ma, meaning that the transition would have occurred earlier there. Some clustering of age data suggests volcanism over the past 1 Ma was episodic, with some periods of dominantly felsic eruptions, notably at 0.8–0.65 Ma. Monogenetic volcanoes located close together in Syunik often have a similar age, indicating a future eruption is particularly likely close to the young Karkar lava flow field. A lava flow from one of the Holocene eruptions at Karkar came within 5 km of the modern road link between Armenia and Iran, and if a future eruption were to block this road it could cause substantial disruption to regional infrastructure.

With an average rate of 1.6×10^{-4} eruptions/year in Syunik, the frequency of eruptions is at the upper end of the observed range for volcanic fields globally. A relatively high magma flux is consistent with the presence of abundant felsic eruptive products. The high eruption rate observed in Syunik makes a decreasing magma supply a strong candidate for what drove the polygenetic to monogenetic transition. A past eruption rate which was an order of magnitude higher than the average for the past 1 Ma would likely have been sufficient to facilitate the formation of polygenetic volcanoes. Several lines of evidence suggest the polygenetic to monogenetic transition in Syunik reflected a waning magma supply: (i) estimates of the volumes of lava erupted suggests the output rate has decreased with time; (ii) the transition occurred last in Syunik, which also has the highest density of vents, suggesting the highest magma flux, and therefore it should be the last place in the region where volcanism would transition to a monogenetic mode; and (iii) field observations from the wider Lesser Caucasus region reveal a transition in the style of volcanism from large volume flood basalt eruptions, through the formation of several large polygenetic volcanoes

(capable of producing multiple massive ignimbrite sheets), to small volume scoria cone eruptions.

The close association of pull-apart basin structures with volcanism gives the impression that the localised extension promotes the development of monogenetic volcanism. The clusters of volcanoes with similar ages probably reflect old pull-apart basins where melt was once focussed. While some of youngest volcanoes, such as those at Karkar have formed in pull-apart structures, other young late Pleistocene-Holocene volcanoes which are more isolated from other vents, such as Vayots-Sar and Smbatasar, are not associated with a pull-apart basin. This suggests that while magmas may exploit normal faults as favourable pathways for magma ascent, they are not a requisite for volcanic activity. These isolated Holocene volcanoes show that although future volcanic activity may be particularly likely close to recent hotspots such as Karkar, there is also a possibility for new vents to form in more unexpected places. The constant deformation rates seen for Lesser Caucasus faults during the Pleistocene demonstrates that an increase in crustal extension rates is unlikely to have been the cause of the polygenetic to monogenetic transition in Syunik.

Despite waning volcanic activity, there is a lack of geochemical variation with time, suggesting the slab component in the mantle source is not being exhausted, and that the lithospheric mantle is capable of preserving slab signatures for millions of years after the end of subduction. Current volcanic activity is likely to represent the end of a magmatic pulse, probably initiated by a heating event, perhaps delamination in the mantle lithosphere. The sustained slab component in the mantle source suggests that on geological timescales, future pulses of volcanism are likely in the Arabia-Eurasia collision zone.

Declaration of Competing Interest

None.

Acknowledgements

This paper is dedicated to Sergei Karapetian and to Arkadi Karakhanian- the tireless and enthusiastic early explorers of these vast and beautiful landscapes. The authors would like to thank the rest of the fieldwork team who collected the samples in the Vardenis and Syunik volcanic highlands including Ralf Halama, Krzysztof Sokół, Samuele Agostini, Laura Connor, and the IGS-Yerevan staff including our heroic off-road drivers Hayrapet Palandiyan, Gagik Sargsyan, Martin Gasparyan, and Marat Yeritsyan. Argon isotopic analyses were funded by NERC grant to I. Savov, IP-1690-1116. PJS would like to thank all the scientists at SUERC who provided a helping hand during sample preparation, in particular Ross Dymock. PJS was funded through a NERC studentship as part of the Leeds York Spheres Doctoral Training Partnership (DTP) (grant number NE/L002574/1). We would also like to thank Laura Connor for her help with gmt when producing the vent density map. For their helpful discussions we would like to also thank Dan Morgan, Julian Pearce, Ruben Jrbashian and Iain Neill. Part of the field work and research were supported by base funding of the Institute of Geological Sciences (IGS) and a thematic project by the Science Committee of the Armenian Ministry of Education and Science (project #18 T-1E368).

Appendix A. Supplementary data

Supplementary data to this article can be found online at https://doi.org/10.1016/j.jvolgeores.2021.107192.

References

Allen, M.B., Kheirkhah, M., Neill, I., Emami, M.H., McLeod, C.L., 2013. Generation of arc andwithin-plate chemical signatures in collision zone magmatism: Quaternary lavas from kurdistan province. Iran. J. Petrol. 54, 887–911. https://doi.org/10.1093/petrology/egs090.

Arce, J.L., Layer, P.W., Lassiter, J.C., Benowitz, J.A., Macías, J.L., Ramírez-Espinosa, J., 2013. 40Ar/39Ar dating, geochemistry, and isotopic analyses of the quaternary Chichinautzin volcanic field, south of Mexico City: Implications for timing, eruption rate, and distribution of volcanism. Bull. Volcanol. 75, 774. https://doi.org/10.1007/s00445-013-0774-6.

Arutyunyan, E.V., Lebedev, V.A., Chernyshev, I.V., Sagatelyan, A.K., 2007. Geochronology of Neogene-Quaternary volcanism of the Geghama Highland (Lesser Caucasus, Armenia). Dokl. Earth Sci. 416, 1042–1046. https://doi.org/10.1134/S1028334X07070136.

Belousov, A., Belousova, M., Edwards, B., Volynets, A., Melnikov, D., 2015. Overview of the precursors and dynamics of the 2012-13 basaltic fissure eruption of Tolbachik Volcano, Kamchatka, Russia. J. Volcanol. Geotherm. Res. 307, 22–37. https://doi.org/10.1016/j.jvolgeores.2015.06.013.

Bertin, D., Lindsay, J.M., Becerril, L., Cronin, S.J., Bertin, L.J., 2019. MatHaz: a Matlab code to assist with probabilistic spatio-temporal volcanic hazard assessment in distributed volcanic fields. J. Appl. Volcanol. 8, 4. https://doi.org/10.1186/s13617-019-0084-6.

Bucchi, F., Lara, L.E., Gutiérrez, F., 2015. The Carrán-Los Venados volcanic field and its relationship with coeval and nearby polygenetic volcanism in an intra-arc setting. J. Volcanol. Geotherm. Res. 308, 70–81. https://doi.org/10.1016/j.jvolgeores.2015.10.013.

Chernyshev, I.V., Lebedev, V.A., Arakelyants, R.T., Jrbashian, R.T., Ghukasyan, Y., 2002. Geochronology of the Aragats volcanic Centre, Armenia: evidence from K-Ar dating. Dokl. Earth Sci. 384, 393–398.

Connor, C.B., Conway, F.M., 2000. Basaltic Volcanic Fields. In: Sigurdsson, H., Houghton, B., McNutt, S.R., Rymer, H., Stix, J. (Eds.), Encyclopedia of Volcanoes. Academic Press, San Diego, USA; Waltham, USA, pp. 331–343.

Connor, C.B., Connor, L., Halama, R., Meliksetian, K., Savov, I., 2011. Volcanic Hazard Assessment of the Armenia Nuclear Power Plant Site, Final Report. Tampa, FL, USA; Leeds, UK; Yerevan, Armenia.

Connor, L.J., Connor, C.B., Meliksetian, K., Savov, I., 2012. Probabilistic approach to modeling lava flow inundation: a lava flow hazard assessment for a nuclear facility in Armenia. J. Appl. Volcanol. 1, 3. https://doi.org/10.1186/2191-5040-1-3.

Connor, C.B., Connor, L., Germa, A., Richardson, J., Bebbington, M., Gallant, E., Saballos, A., 2019. How to use kernel density estimation as a diagnostic and forecasting tool for distributed volcanic vents. Stat. Volcanol. 4, 1–25. https://doi.org/10.5038/2163-338x.4.3.

Dóniz-Páez, J., 2015. Volcanic geomorphological classification of the cinder cones of Tenerife (Canary Islands, Spain). Geomorphology 228, 432–447. https://doi.org/10.1016/j.geomorph.2014.10.004.

Duong, T., Hazelton, M.L., 2003. Plug-in bandwidth matrices for bivariate kernel density estimation. J. Nonparametr. Stat. 15, 17–30. https://doi.org/10.1080/10485250306039.

Fedotov, S.A., 1981. Magma rates in feeding conduits of different volcanic centres. J. Volcanol. Geotherm. Res. 9, 379–394. https://doi.org/10.1016/0377-0273(81)90045-7.

Foshag, W.F., González Reyna, J., 1956. Birth and development of Paricutin volcano. Mexico. US Geol. Surv. Bull. 965, 355–489.

Germa, A., Connor, L.J., Cañon-Tapia, E., Le Corvec, N., 2013. Tectonic and magmatic controls on the location of post-subduction monogenetic volcanoes in Baja California, Mexico, revealed through spatial analysis of eruptive vents. Bull. Volcanol. 75, 782. https://doi.org/10.1007/s00445-013-0782-6.

Germa, A., Perry, C., Quidelleur, X., Calvert, A., Clynne, M., Connor, C.B., Connor, L.J., Malservisi, R., Charbonnier, S., 2019. Temporal relationship between the Lassen volcanic center and mafic regional volcanism. Bull. Volcanol. 81, 38. https://doi.org/10.1007/s00445-019-1296-7.

Gevorgyan, H., Repstock, A., Schulz, B., Meliksetian, K., Breitkreuz, C., Israyelyan, A., 2018. Decoding a post-collisional multistage magma system: the Quaternary ignimbrites of Aragats stratovolcano, western Armenia. Lithos 318, 267–282. https://doi.org/10.1016/j.lithos.2018.07.024.

Gevorgyan, H., Breitkreuz, C., Meliksetian, K., Israyelyan, A., Ghukasyan, Y., Pfänder, J.A., Sperner, B., Miggins, D.P., Koppers, A., 2020. Quaternary ring plain- and valley-confined pyroclastic deposits of Aragats stratovolcano (Lesser Caucasus): Lithofacies, geochronology and eruption history. J. Volcanol. Geotherm. Res. 401, 106928. https://doi.org/10.1016/j.jvolgeores.2020.106928.

Ghalamghash, J., Mousavi, S.Z., Hassanzadeh, J., Schmitt, A.K., 2016. Geology, zircon geochronology, and petrogenesis of Sabalan volcano (northwestern Iran). J. Volcanol. Geotherm. Res. 327, 192–207. https://doi.org/10.1016/j.jvolgeores.2016.05.001.

Ghukasyan, Y., 1985. Petrography, Mineralogical-Geochemical Characteristics and the History of the Forming of Aragats Volcanic Complex. Academy of Sciences, Yereven, Armenian SSR.

Gilliland, J., Austin, A., Shibesh, K., Wilmarth, M., Daskin, C., Babaya, T., 2018. Karkar, Armenia Slimehole drilling and testing results and remote project management overview. Proceedings, African Rift Geothermal Conference, Kigali, Rwanda. Kigali, Rwanda.

Gómez-Vasconcelos, M.G., Luis Macías, J., Avellán, D.R., Sosa-Ceballos, G., Garduño-Monroy, V.H., Cisneros-Máximo, G., Layer, P.W., Benowitz, J., López-Loera, H., López, F.M., Perton, M., 2020. The control of preexisting faults on the distribution, morphology, and volume of monogenetic volcanism in the Michoacán-Guanajuato Volcanic Field. Geol. Soc. Am. Bull. https://doi.org/10.1130/b35397.1.

Hasebe, N., Fukutani, A., Sudo, M., Tagami, T., 2001. Transition of eruptive style in an arc-arc collision zone: K-Ar dating of Quaternary monogenetic and polygenetic volcanoes in the Higashi-Izu region, Izu peninsula, Japan. Bull. Volcanol. 63, 377–386. https://doi.org/10.1007/s004450100158.

Hickey-Vargas, R., Sun, M., López-Escobar, L., Moreno-Roa, H., Reagan, M.K., Morris, J.D., Ryan, J.G., 2002. Multiple subduction components in the mantle wedge: evidence from eruptive centers in the Central Southern volcanic zone, Chile. Geology 30, 199–202. https://doi.org/10.1130/0091-7613(2002)030<0199:mscitm>2.0.co;2.

Hildreth, W., 2007. Quaternary magmatism in the Cascades - Geologic perspectives. US Geol. Surv. Prof. Pap. https://doi.org/10.3133/pp1744.

IAEA-TECDOC-1795, Aspinall, W., Charbonnier, S., Connor, C.B., Connor, L.J., Costa, A., Courtland, L., Delgado Granados, H., Hibino, K., Hill, B., Komorowski, J.C., McNutt, S.,

Meliksetian, K., Nakada, S., Newhall, C., Samaddar, S., Savov, I.P., Self, S., Uchiyamer, Y., Wilson, T., Yamamoto, T., 2016. Volcanic Hazard Assessment for Nuclear Installations: Methods and Examples in Site Evaluation. 1795. International Atomic Energy Agency TECDOC series.

Joannin, S., Cornée, J.-J., Münch, P., Fornari, M., Vasiliev, I., Krijgsman, W., Nahapetyan, S., Gabrielyan, I., Ollivier, V., Roiron, P., Chataigner, C., 2010. Early Pleistocene climate cycles in continental deposits of the Lesser Caucasus of Armenia inferred from palynology, magnetostratigraphy, and 40Ar/39Ar dating. Earth Planet. Sci. Lett. 291, 149–158. https://doi.org/10.1016/j.epsl.2010.01.007.

Kaislaniemi, L., van Hunen, J., Allen, M.B., Neill, I., 2014. Sublithospheric small-scale convection–a mechanism for collision zone magmatism. Geology 42, 291–294. https://doi.org/10.1130/G35193.1.

Karakhanian, A., Djrbashian, R., Trifonov, V., Philip, H., Arakelian, S., Avagian, A., 2002. Holocene-historical volcanism and active faults as natural risk factors for Armenia and adjacent countries. J. Volcanol. Geotherm. Res. 113, 319–344. https://doi.org/10.1016/S0377-0273(01)00264-5.

Karakhanian, A., Jrbashyan, R., Trifonov, V., Philip, H., Arakelian, S., Avagyan, A., Baghdassaryan, H., Davtian, V., Ghoukassyan, Y., 2003. Volcanic hazards in the region of the Armenian Nuclear Power Plant. J. Volcanol. Geotherm. Res. 126, 31–62. https://doi.org/10.1016/S0377-0273(03)00115-X.

Karakhanyan, A., Vernant, P., Doerflinger, E., Avagyan, A., Philip, H., Aslanyan, R., Champollion, C., Arakelyan, S., Collard, P., Baghdasaryan, H., Peyret, M., Davtyan, V., Calais, E., Masson, F., 2013. GPS constraints on continental deformation in the Armenian region and Lesser Caucasus. Tectonophysics 592, 39–45. https://doi.org/10.1016/j.tecto.2013.02.002.

Karakhanyan, A., Arakelyan, A., Avagyan, A., Sadoyan, T., 2016. Aspects of the seismotectonics of Armenia : New data and reanalysis. In: Sorkhabi, R. (Ed.), Tectonic Evolution, Collision and Seismicity of Southwest Asia: In Honour of Manuel Berberian's Forty Five Years of Research Contributions. Geological Society of America Special Paper. vol. 525, pp. 445–477. https://doi.org/10.1130/2016.2525(14).

Karapetian, S.G., Jrbashian, R.T., Mnatsakanian, A.K., 2001. Late collision rhyolitic volcanism in the north-eastern part of the Armenian highland. J. Volcanol. Geotherm. Res. 112, 189–220. https://doi.org/10.1016/S0377-0273(01)00241-4.

Keskin, M., 2003. Magma generation by slab steepening and breakoff beneath a subduction-accretion complex: an alternative model for collision-related volcanism in Eastern Anatolia. Turkey. Geophys. Res. Lett. 30, 8046. https://doi.org/10.1029/2003GL018019.

Keskin, M., Pearce, J.A., Mitchell, J.G., 1998. Volcano-stratigraphy and geochemistry of collision-related volcanism on the Erzurum-Kars Plateau, northeastern Turkey. J. Volcanol. Geotherm. Res. 85, 355–404. https://doi.org/10.1016/S0377-0273(98)00063-8.

Keskin, M., Pearce, J.A., Pavlides, S., Greenwood, P., Kempton, P.D., Dilek, Y., 2006. Magma-crust interactions and magma plumbing in a postcollisional setting: Geochemical evidence from the Erzurum-Kars volcanic plateau, eastern Turkey. Geol. Soc. Am. Spec. Pap. 409, 475–505. https://doi.org/10.1130/2006.2409(23).

Kiyosugi, K., Connor, C.B., Zhao, D., Connor, L.J., Tanaka, K., 2010. Relationships between volcano distribution, crustal structure, and P-wave tomography: an example from the Abu Monogenetic Volcano Group, SW Japan. Bull. Volcanol. 72, 331–340. https://doi.org/10.1007/s00445-009-0316-4.

Kiyosugi, K., Connor, C.B., Wetmore, P.H., Ferwerda, B.P., Germa, A.M., Connor, L.J., Hintz, A.R., 2012. Relationship between dike and volcanic conduit distribution in a highly eroded monogenetic volcanic field: San Rafael, Utah, USA. Geology 40, 695–698. https://doi.org/10.1130/G33074.1.

Lebedev, V.A., Chernyshev, I.V., Shatagin, K.N., Bubnov, S.N., Yakushev, A.I., 2013. The quaternary volcanic rocks of the Geghama highland, Lesser Caucasus, Armenia: Geochronology, isotopic Sr-Nd characteristics, and origin. J. Volcanol. Seismol. 7, 204–229. https://doi.org/10.1134/S0742046313030044.

Luhr, J.F., Navarro-Ochoa, C., Savov, I.P., 2010. Tephrochronology, petrology and geochemistry of Late-Holocene pyroclastic deposits from Volcán de Colima, Mexico. J. Volcanol. Geotherm. Res. 197, 1–32. https://doi.org/10.1016/j.jvolgeores.2009.11.007.

Mark, D.F., Barfod, D., Stuart, F.M., Imlach, J., 2009. The ARGUS multicollector noble gas mass spectrometer: Performance for 40Ar/39Ar geochronology. Geochem. Geophys. Geosyst. 10. https://doi.org/10.1029/2009GC002643 Q0AA02.

Mazzarini, F., Isola, I., 2010. Monogenetic vent self-similar clustering in extending continental crust: examples from the East African Rift System. Geosphere 6, 567–582. https://doi.org/10.1130/GES00569.1.

Meliksetian, K., 2013. Pliocene-Quaternary volcanism of the Syunik upland. Archaol. Armen. II 67, 247–258.

Meliksetian, K., Neill, I., Barfod, D.N., Milne, E., Waters, E., Navasardyan, G., Olive, V., Odling, N., 2020. Pleistocene - Holocene volcanism at the Karkar geothermal prospect, Armenia. EarthArXiv Prepr. https://doi.org/10.31223/osf.io/x3tpg.

Mitchell, J., Westaway, R., 1999. Chronology of Neogene and Quaternary uplift and magmatism in the Caucasus: constraints from K-Ar dating of volcanism in Armenia. Tectonophysics 304, 157–186. https://doi.org/10.1016/S0040-1951(99)00027-X.

Muirhead, J.D., Van Eaton, A.R., Re, G., White, J.D.L., Ort, M.H., 2016. Monogenetic volcanoes fed by interconnected dikes and sills in the Hopi Buttes volcanic field, Navajo Nation, USA. Bull. Volcanol. 78, 11. https://doi.org/10.1007/s00445-016-1005-8.

Nagaoka, S., Okuno, M., 2011. Tephrochronology and eruptive history of Kirishima volcano in southern Japan. Quat. Int. 246, 260–269. https://doi.org/10.1016/j.quaint.2011.06.007.

Nakamura, K., 1977. Volcanoes as possible indicators of tectonic stress orientation - principle and proposal. J. Volcanol. Geotherm. Res. 2, 1–16. https://doi.org/10.1016/0377-0273(77)90012-9.

Neill, I., Meliksetian, K., Allen, M.B., Navarsardyan, G., Karapetyan, S., 2013. Pliocene-Quaternary volcanic rocks of NW Armenia: Magmatism and lithospheric dynamics within an active orogenic plateau. Lithos 180, 200–215. https://doi.org/10.1016/j.lithos.2013.05.005.

Neill, I., Meliksetian, K., Allen, M.B., Navasardyan, G., Kuiper, K., 2015. Petrogenesis of mafic collision zone magmatism: the Armenian sector of the Turkish–Iranian Plateau. Chem. Geol. 403, 24–41. https://doi.org/10.1016/j.chemgeo.2015.03.013.

Niespolo, E.M., Rutte, D., Deino, A.L., Renne, P.R., 2017. Intercalibration and age of the Alder Creek sanidine 40Ar/39Ar standard. Quat. Geochronol. 39, 205–213. https://doi.org/10.1016/j.quageo.2016.09.004.

Ollivier, V., Nahapetyan, S., Roiron, P., Gabrielyan, I., Gasparyan, B., Chataigner, C., Joannin, S., Cornée, J.J., Guillou, H., Scaillet, S., Munch, P., Krijgsman, W., 2010. Quaternary volcano-lacustrine patterns and palaeobotanical data in southern Armenia. Quat. Int. 223, 312–326. https://doi.org/10.1016/j.quaint.2010.02.008.

Philip, H., Avagyan, A., Karakhanian, A., Ritz, J.F., Rebai, S., 2001. Estimating slip rates and recurrence intervals for strong earthquakes along an intracontinental fault: example of the Pambak-Sevan-Sunik fault (Armenia). Tectonophysics 343, 205–232. https://doi.org/10.1016/S0040-1951(01)00258-X.

Reubi, O., Blundy, J., 2009. A dearth of intermediate melts at subduction zone volcanoes and the petrogenesis of arc andesites. Nature 461, 1269–1273. https://doi.org/10.1038/nature08510.

Reynolds, P., Schofield, N., Brown, R.J., Holford, S.P., 2018. The architecture of submarine monogenetic volcanoes – insights from 3D seismic data. Basin Res. 30, 437–451. https://doi.org/10.1111/bre.12230.

Riggs, N., Ort, M.H., Connor, C.B., Alfano, F., Conway, M., 2019. Volcanology and associated hazards of the San Francisco volcanic field. In: Pearthree, P.A. (Ed.), Geologic Excursions in Southwestern North America: Geological Society of America Field Guide 55. Geological Society of America, pp. 127–146.

Rittmann, A., 1962. Volcanoes and their Activity. John Wiley and Sons, New York.

Sargsyan, L., Meliksetian, K., Metaxian, J.-P., Levonyan, A., Karakhanyan, A., Demirchyan, H., Navasardyan, G., Margaryan, S., Gevorgyan, M., Babayan, H., 2018. Preliminary results of analysis of earthquake swarms in Gegham volcanic ridge. EGU General Assembly Conference Abstracts. Vol. 20. EGU, Vienna, p. 417.

Şengör, A.M.C., Özeren, M.S., Keskin, M., Sakinç, M., Özbakir, A.D., Kayan, I., 2008. Eastern Turkish high plateau as a small Turkic-type orogen: Implications for post-collisional crust-forming processes in Turkic-type orogens. Earth-Sci. Rev. 90, 1–48. https://doi.org/10.1016/j.earscirev.2008.05.002.

Settle, M., 1979. The structure and emplacement of cinder cone fields. Am. J. Sci. 279, 1089–1107. https://doi.org/10.2475/ajs.279.10.1089.

Sheth, H., Meliksetian, K., Gevorgyan, H., Israyelyan, A., Navasardyan, G., 2015. Intracanyon basalt lavas of the Debed River (northern Armenia), part of a Pliocene–Pleistocene continental flood basalt province in the South Caucasus. J. Volcanol. Geotherm. Res. 295, 1–15. https://doi.org/10.1016/j.jvolgeores.2015.02.010.

Sieron, Katrin, Ferres, D., Siebe, C., Capra, L., Constantinescu, R., Agustín-Flores, J., González Zuccolotto, K., Böhnel, H., Connor, L., Connor, C.B., Groppelli, G., 2019a. Ceboruco hazard map: Part i - Definition of hazard scenarios based on the eruptive history. J. Appl. Volcanol. 9, 1–22. https://doi.org/10.1186/s13617-019-0088-2.

Sieron, K., Ferrés, D., Siebe, C., Constantinescu, R., Capra, L., Connor, C., Connor, L., Groppelli, G., González Zuccolotto, K., 2019b. Ceboruco hazard map: part II—modeling volcanic phenomena and construction of the general hazard map. Nat. Hazards 96, 893–933. https://doi.org/10.1007/s11069-019-03577-5.

Smith, I.E.M., Németh, K., 2017. Source to surface model of monogenetic volcanism: A critical review. In: Németh, K., Carrasco-Núñez, G., Aranda-Gómez, J.J., Smith, I.E.M. (Eds.), Monogenetic Volcanism. Geological Society, London, Special Publications, London, pp. 1–28 https://doi.org/10.1144/sp446.14.

Sparks, R.S.J., Folkes, C.B., Humphreys, M.C.S., Barfod, D.N., Clavero, J., Sunagua, M.C., McNutt, S.R., Pritchard, M.E., 2008. Uturuncu volcano, Bolivia: Volcanic unrest due to mid-crustal magma intrusion. Am. J. Sci. 308, 727–769. https://doi.org/10.2475/06.2008.01.

Sparks, R.S.J., Annen, C., Blundy, J.D., Cashman, K.V., Rust, A.C., Jackson, M.D., 2019. Formation and dynamics of magma reservoirs. Philos. Trans. R. Soc. A Math. Phys. Eng. Sci. 377, 20180019. https://doi.org/10.1098/rsta.2018.0019.

Sugden, P.J., Savov, I.P., Wilson, M., Meliksetian, K., Navasardyan, G., Halama, R., 2019. The Thickness of the Mantle Lithosphere and Collision-related Volcanism in the Lesser Caucasus. J. Petrol. 60, 199–230.

Sugden, P.J., Savov, I.P., Agostini, S., Wilson, M., Halama, R., Meliksetian, K., 2020. Boron isotope insights into the origin of subduction signatures in continent-continent collision zone volcanism. Earth Planet. Sci. Lett. 538, 116207. https://doi.org/10.1016/j.epsl.2020.116207.

Takada, A., 1994a. The influence of regional stress and magmatic input on styles of monogenetic and polygenetic volcanism. J. Geophys. Res. Solid Earth 99, 13563–13573. https://doi.org/10.1029/94jb00494.

Takada, A., 1994b. Development of a subvolcanic structure by the interaction of liquid-filled cracks. J. Volcanol. Geotherm. Res. 62, 207–224. https://doi.org/10.1016/0377-0273(94)90004-3.

Thordarson, T., Larsen, G., 2007. Volcanism in Iceland in historical time: Volcano types, eruption styles and eruptive history. J. Geodyn. 43, 118–152. https://doi.org/10.1016/j.jog.2006.09.005.

Valentine, G.A., Connor, C.B., 2015. Basaltic Volcanic Fields. In: Sigurdsson, H. (Ed.), The Encyclopedia of Volcanoes. Academic Press, San Diego, USA; Waltham, USA, pp. 423–439 https://doi.org/10.1016/b978-0-12-385938-9.00023-7.

Walker, G.P.L., 1993. Basaltic-volcano systems. In: Prichard, H.M., Alabaster, T., Harris, N.B.W., Neary, C.R. (Eds.), Magmatic Processes and Plate Tectonics. Geological Society Special Publication no. 76, London, pp. 3–38 https://doi.org/10.1144/GSL.SP.1993.076.01.01.

Walker, J.A., Singer, B.S., Jicha, B.R., Cameron, B.I., Carr, M.J., Olney, J.L., 2011. Monogenetic, behind-the-front volcanism in southeastern Guatemala and western El Salvador:

40Ar/39Ar ages and tectonic implications. Lithos 123, 243–253. https://doi.org/10.1016/j.lithos.2010.09.016.
White, J.T., Karakhanian, A., Connor, C.B., Connor, L., Hughes, J.D., Malservisi, R., Wetmore, P., 2015. Coupling geophysical investigation with hydrothermal modeling to constrain the enthalpy classification of a potential geothermal resource. J. Volcanol. Geotherm. Res. 298, 59–70. https://doi.org/10.1016/j.jvolgeores.2015.03.020.
Yilmaz, Y., Güner, Y., Şaroglu, F., 1998. Geology of the quaternary volcanic centres of the East Anatolia. J. Volcanol. Geotherm. Res. 85, 173–210. https://doi.org/10.1016/S0377-0273(98)00055-9.
Yokoyama, I., 2019. Clusters of small monogenetic cones: a particular type of confined volcanism. Ann. Geophys. 62 (V), 0678. https://doi.org/10.4401/ag-8176.
Zou, H., Guo, Z., Peng, Y., Schmitt, A.K., Fan, Q., Zhao, Y., Ma, M., 2020a. U-series ages of young volcanoes from the Southeastern Tibetan Plateau: Holocene eruptions and magma evolution timescales. Lithos 370–371, 105643. https://doi.org/10.1016/j.lithos.2020.105643.
Zou, H., Vazquez, J., Fan, Q., 2020b. Timescales of magmatic processes in post-collisional potassic lavas, northwestern Tibet. Lithos 358–359, 105418. https://doi.org/10.1016/j.lithos.2020.105418.